Since January 2020 Elsevier has created a COVID-19 resource centre with free information in English and Mandarin on the novel coronavirus COVID-19. The COVID-19 resource centre is hosted on Elsevier Connect, the company's public news and information website.

Cell

mRNA-1273 or mRNA-Omicron boost in vaccinated macaques elicits similar B cell expansion, neutralizing responses, and protection from Omicron

Graphical abstract

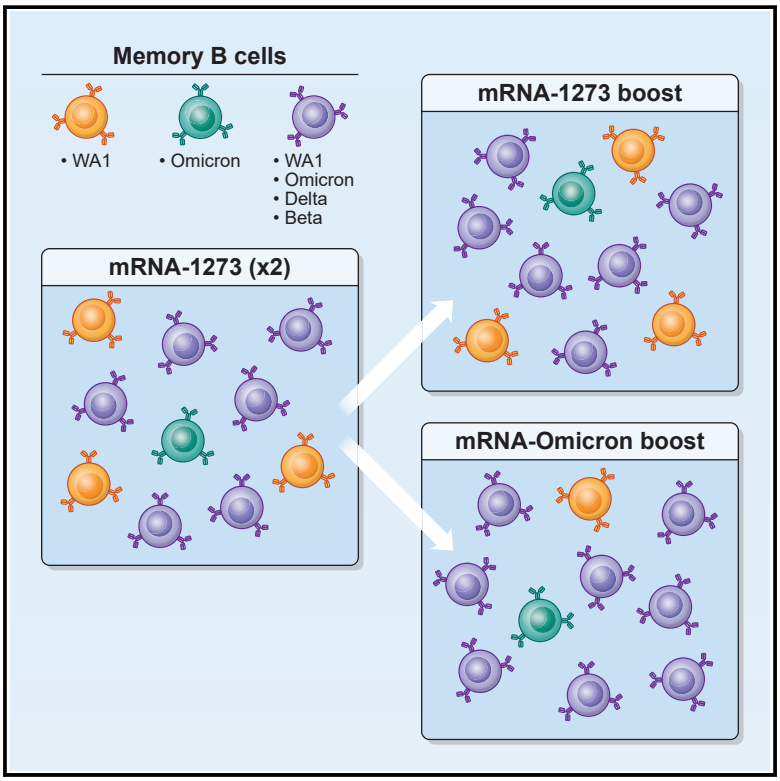

Highlights

- mRNA-1273 prime induces cross-reactive B cells to Omicron and ancestral strains
- Boosting with mRNA-1273 or mRNA-Omicron enhances neutralization of Omicron
- Either boost expands B cells cross-reactive to Omicron and ancestral strains
- mRNA-1273 or mRNA-Omicron boost is protective against Omicron replication in the lungs

Authors

Matthew Gagne, Juan I. Moliva, Kathryn E. Foulds, ..., Nancy J. Sullivan, Daniel C. Douek, Robert A. Seder

Correspondence

ddouek@mail.nih.gov (D.C.D.), rseder@mail.nih.gov (R.A.S.)

In brief

Boosting previously vaccinated nonhuman primates with either the mRNA-1273 or mRNA-Omicron vaccine expands cross-reactive memory B cells and elicits similar levels of protection upon challenge with SARS-CoV-2 Omicron.

Gagne et al., 2022, Cell *185*, 1556–1571
April 28, 2022 Published by Elsevier Inc.
https://doi.org/10.1016/j.cell.2022.03.038

CellPress

CellPress

Cell

Article

mRNA-1273 or mRNA-Omicron boost in vaccinated macaques elicits similar B cell expansion, neutralizing responses, and protection from Omicron

Matthew Gagne,[1,9] Juan I. Moliva,[1,9] Kathryn E. Foulds,[1,9] Shayne F. Andrew,[1,9] Barbara J. Flynn,[1,9] Anne P. Werner,[1,9] Danielle A. Wagner,[1,9] I-Ting Teng,[1] Bob C. Lin,[1] Christopher Moore,[1] Nazaire Jean-Baptiste,[1] Robin Carroll,[1] Stephanie L. Foster,[2] Mit Patel,[2] Madison Ellis,[2] Venkata-Viswanadh Edara,[2] Nahara Vargas Maldonado,[2] Mahnaz Minai,[3] Lauren McCormick,[1] Christopher Cole Honeycutt,[1] Bianca M. Nagata,[3] Kevin W. Bock,[3] Caitlyn N.M. Dulan,[1] Jamilet Cordon,[1] Dillon R. Flebbe,[1] John-Paul M. Todd,[1] Elizabeth McCarthy,[1] Laurent Pessaint,[4] Alex Van Ry,[4] Brandon Narvaez,[4] Daniel Valentin,[4] Anthony Cook,[4] Alan Dodson,[4] Katelyn Steingrebe,[4] Saule T. Nurmukhambetova,[1] Sucheta Godbole,[1] Amy R. Henry,[1] Farida Laboune,[1] Jesmine Roberts-Torres,[1] Cynthia G. Lorang,[1] Shivani Amin,[1] Jessica Trost,[1] Mursal Naisan,[1] Manjula Basappa,[1] Jacquelyn Willis,[1] Lingshu Wang,[1] Wei Shi,[1] Nicole A. Doria-Rose,[1] Yi Zhang,[1] Eun Sung Yang,[1] Kwanyee Leung,[1] Sijy O'Dell,[1] Stephen D. Schmidt,[1] Adam S. Olia,[1] Cuiping Liu,[1] Darcy R. Harris,[1] Gwo-Yu Chuang,[5] Guillaume Stewart-Jones,[5] Isabella Renzi,[5] Yen-Ting Lai,[5] Agata Malinowski,[5] Kai Wu,[5] John R. Mascola,[1] Andrea Carfi,[5] Peter D. Kwong,[1] Darin K. Edwards,[5] Mark G. Lewis,[4] Hanne Andersen,[4] Kizzmekia S. Corbett,[6] Martha C. Nason,[7] Adrian B. McDermott,[1] Mehul S. Suthar,[2] Ian N. Moore,[8] Mario Roederer,[1] Nancy J. Sullivan,[1] Daniel C. Douek,[1,*] and Robert A. Seder[1,10,*]

[1]Vaccine Research Center, National Institute of Allergy and Infectious Diseases, National Institutes of Health, Bethesda, MD 20892, USA
[2]Department of Pediatrics, Emory Vaccine Center, Yerkes National Primate Research Center, Emory University School of Medicine, Atlanta, GA 30322, USA
[3]Infectious Disease Pathogenesis Section, Comparative Medicine Branch, National Institute of Allergy and Infectious Diseases, National Institutes of Health, Rockville, MD 20892, USA
[4]Bioqual, Inc., Rockville, MD 20850, USA
[5]Moderna Inc., Cambridge, MA 02139, USA
[6]Department of Immunology and Infectious Diseases, Harvard T.H. Chan School of Public Health, Boston, MA 02115, USA
[7]Biostatistics Research Branch, Division of Clinical Research, National Institute of Allergy and Infectious Diseases, National Institutes of Health, Bethesda, MD 20892, USA
[8]Division of Pathology, Yerkes National Primate Research Center, Emory University School of Medicine, Atlanta, GA 30329, USA
[9]These authors contributed equally
[10]Lead contact
*Correspondence: ddouek@mail.nih.gov (D.C.D.), rseder@mail.nih.gov (R.A.S.)
https://doi.org/10.1016/j.cell.2022.03.038

SUMMARY

SARS-CoV-2 Omicron is highly transmissible and has substantial resistance to neutralization following immunization with ancestral spike-matched vaccines. It is unclear whether boosting with Omicron-matched vaccines would enhance protection. Here, nonhuman primates that received mRNA-1273 at weeks 0 and 4 were boosted at week 41 with mRNA-1273 or mRNA-Omicron. Neutralizing titers against D614G were 4,760 and 270 reciprocal ID_{50} at week 6 (peak) and week 41 (preboost), respectively, and 320 and 110 for Omicron. 2 weeks after the boost, titers against D614G and Omicron increased to 5,360 and 2,980 for mRNA-1273 boost and 2,670 and 1,930 for mRNA-Omicron, respectively. Similar increases against BA.2 were observed. Following either boost, 70%–80% of spike-specific B cells were cross-reactive against WA1 and Omicron. Equivalent control of virus replication in lower airways was observed following Omicron challenge 1 month after either boost. These data show that mRNA-1273 and mRNA-Omicron elicit comparable immunity and protection shortly after the boost.

INTRODUCTION

The COVID-19 mRNA vaccines BNT162b2 and mRNA-1273 provide highly effective protection against symptomatic and severe infection with ancestral SARS-CoV-2 (Baden et al., 2021b; Dagan et al., 2021; Pilishvili et al., 2021; Polack et al., 2020). More recently, protective efficacy has declined due to both waning vaccine-elicited immunity (Baden et al., 2021a; Bergwerk et al., 2021; Goldberg et al., 2021) and antigenic shifts in variants of concern (VOC) including B.1.351 (Beta) and B.1.617.2 (Delta)

(Planas et al., 2021; Wang et al., 2021a, 2021b). Importantly, the introduction of a boost after the initial vaccine regimen enhances immunity and vaccine efficacy against symptomatic disease, hospitalization and death across a broad range of age groups (Andrews et al., 2022; Bar-On et al., 2021; Barda et al., 2021; Garcia-Beltran et al., 2022; Pajon et al., 2022). However, the timing and selection of a boost is a major scientific and clinical challenge during this evolving pandemic in which emerging VOC have distinctive patterns of transmission and virulence and against which vaccine-elicited antibody neutralization is reduced.

The most recent VOC, B.1.1.529, henceforth referred to by its WHO designation of Omicron, was first identified in South Africa in November 2021 and was associated with a dramatic increase in COVID-19 cases (Cele et al., 2022; Maslo et al., 2022). Omicron is highly contagious, with a significant transmission advantage compared with Delta, which until recently was the dominant VOC worldwide (Viana et al., 2022). It remains unclear, however, if this advantage is due to differences in cell entry, enrichment in respiratory aerosols, or the ability to evade immunity conferred by vaccination or prior infection. Compared with the ancestral strain, the BA.1 sublineage of Omicron contains more than 30 mutations in the spike (S) gene, including S477N, T478K, E484A, Q493R, G496S, Q498R, N501Y, and Y505H in the receptor binding motif (RBM) alone. Neutralizing antibody titers in sera of individuals recently recovered from previous infection or shortly after immunization with two doses of an mRNA-based COVID-19 vaccine are dramatically reduced to Omicron compared with the ancestral strains Wuhan-Hu-1, USA-WA1/2020 (WA1), and D614G. Numerous studies using both live virus and pseudovirus neutralization assays report a 60- to 80-fold reduction for convalescent sera and a 20- to 130-fold reduction for vaccinee sera (Edara et al., 2022; Hoffmann et al., 2022; Muik et al., 2022; Schmidt et al., 2022). mRNA-1273 vaccine efficacy against breakthrough cases of Omicron in the first few months after immunization has been estimated as 44% in California, USA and 37% in Denmark (Hansen et al., 2021; Tseng et al., 2022), and a complete loss of protection within 6 months (Accorsi et al., 2022). Multiple reports have suggested that Omicron has reduced virulence compared with prior VOC in humans, mice, and hamsters (Davies et al., 2022; Halfmann et al., 2022; Suryawanshi et al., 2022). It is possible that reduced virulence of Omicron may result from preferential replication in the upper airway compared with the lungs, perhaps due to altered cellular tropism not reliant on expression of transmembrane serine protease 2 (TMPRSS2) (Meng et al., 2022; Willett et al., 2022). However, the effect of any reduction in intrinsic viral pathogenicity may be somewhat offset in the context of reduced vaccine efficacy and enhanced virus transmission in human populations worldwide. Together, these data reinforce the value of boosting to limit the extent of infection from Omicron.

Variant-matched boosts have been suggested as a strategy to enhance neutralizing and binding antibody titers to the corresponding VOC beyond the levels conferred by existing FDA-approved boosts, which are homologous to the original ancestral WA1-matched primary vaccine regimen. We previously showed that boosting mRNA-1273 immunized nonhuman primates (NHP) with either mRNA-1273 or a boost matched to the Beta VOC spike (mRNA-1273.351 or mRNA-Beta) resulted in a significant enhancement of neutralizing antibody responses across all VOC tested and an expansion of S-specific memory B cells with ~80%–90% able to bind both WA1 and Beta spikes. Moreover, both boosts provided substantial and similar protection against Beta replication (Corbett et al., 2021a). These NHP data were confirmed in a study in humans that compared an mRNA-1273 boost with mRNA-Beta ~6 months after the participants had received the standard two-dose mRNA-1273 vaccine regimen (Choi et al., 2021). Following either boost, neutralizing titers were substantially increased against D614G and several variants including Beta and were comparable between boost groups. Of note, the level of neutralizing antibodies to Beta after either boost were about 10-fold higher than after the initial vaccination suggesting affinity maturation or epitope focusing of the B cell response. Together, these data suggest that the variant Beta boost did not uniquely enhance immunity or protection compared with existing ancestral strain-matched boosts. However, as Omicron contains more mutations in S compared with Beta and demonstrates even more substantial escape from vaccine-elicited neutralizing antibodies than Beta, it is unclear whether an Omicron-specific boost would provide an additional protective benefit against Omicron infection beyond that of WA1-matched boosts.

The nonhuman primate (NHP) model has been useful for demonstrating immune correlates, mechanisms, and durability of vaccine-elicited protection against SARS-CoV-2 and has been largely predictive for what has been observed in humans in terms of protective efficacy (Corbett et al., 2021b; Gagne et al., 2022; Gilbert et al., 2021). Here, we vaccinated NHP with 100 μg mRNA-1273 at weeks 0 and 4, which is a similar dose and schedule as used in humans. Animals were then boosted about ~9 months later with 50 μg of either a homologous dose of mRNA-1273 or mRNA-1273.529, which is matched to Omicron S (henceforth referred to as mRNA-Omicron). For the duration of these 9 months, we collected sera, bronchoalveolar lavage (BAL), and nasal washes to analyze the kinetics of antibody binding and neutralization as well as the frequency of S-specific B cells for WA1 and Omicron as well as Beta and Delta. Four weeks after boost, NHP were challenged with Omicron. Viral replication in upper and lower airways and lung inflammation were measured to compare boost-elicited protection against Omicron.

RESULTS

Kinetics of serum antibody responses following mRNA-1273 immunization and boost

Indian-origin rhesus macaques (n = 8) were immunized with 100 μg of mRNA-1273 at weeks 0 and 4 (Figure S1A). Sera were collected at weeks 6 (peak) and 41 (memory) to measure immunoglobulin G (IgG) binding to WA1 S and a panel of VOC, including Omicron (Figure 1A). Unless stated otherwise, we used the BA.1 sublineage of Omicron for all analysis. At week 6, we observed a clear hierarchy of binding titers with WA1 > Delta > Beta > Omicron. Geometric mean titers (GMT) to WA1 and Omicron were 8×10^{19} and 3×10^{15} area under the curve (AUC). Antibody titers waned markedly by week 41,

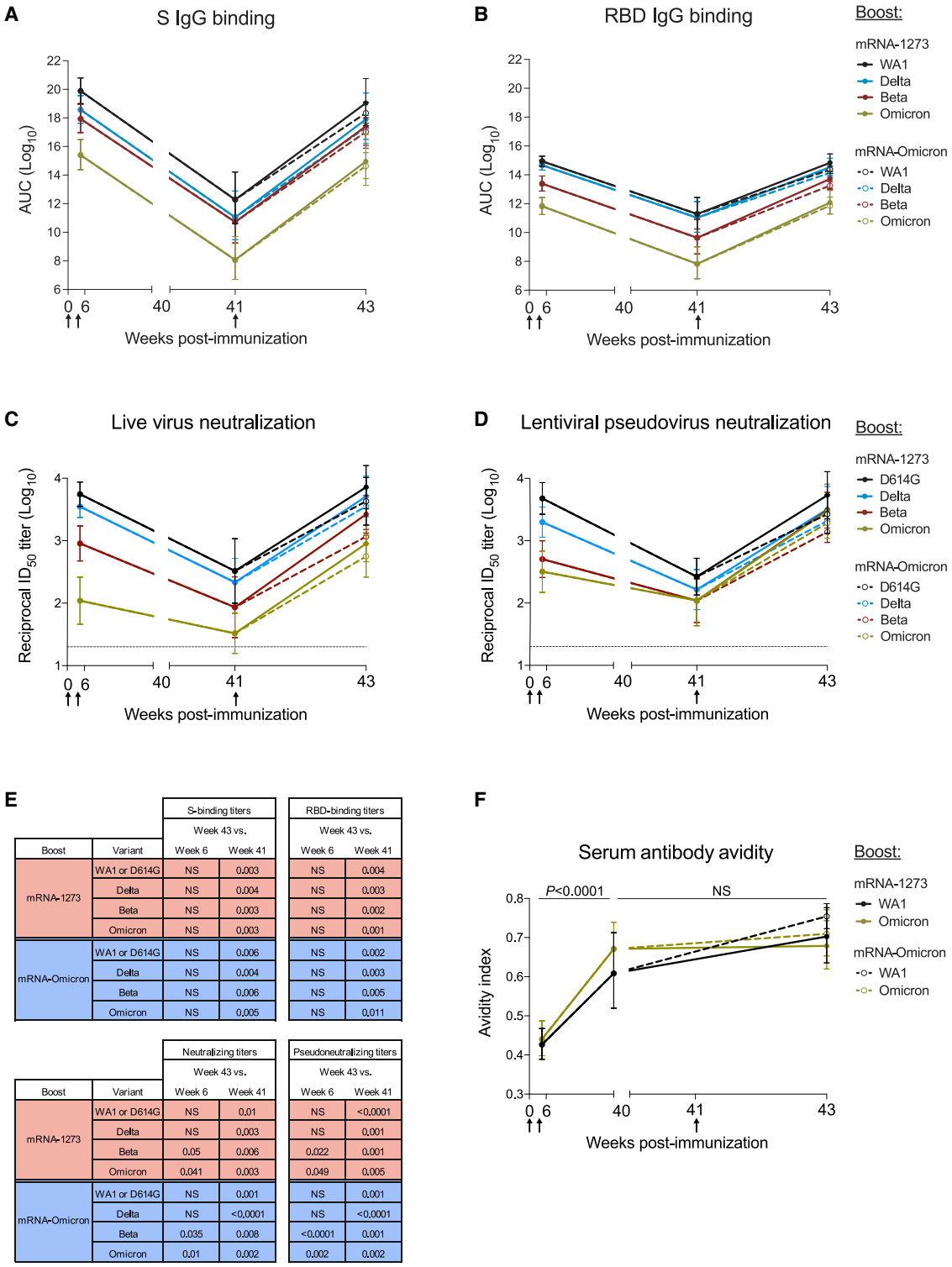

E

Boost	Variant	S-binding titers: Week 43 vs. Week 6	S-binding titers: Week 43 vs. Week 41	RBD-binding titers: Week 43 vs. Week 6	RBD-binding titers: Week 43 vs. Week 41
mRNA-1273	WA1 or D614G	NS	0.003	NS	0.004
	Delta	NS	0.004	NS	0.003
	Beta	NS	0.003	NS	0.002
	Omicron	NS	0.003	NS	0.001
mRNA-Omicron	WA1 or D614G	NS	0.006	NS	0.002
	Delta	NS	0.004	NS	0.003
	Beta	NS	0.006	NS	0.005
	Omicron	NS	0.005	NS	0.011

Boost	Variant	Neutralizing titers: Week 43 vs. Week 6	Neutralizing titers: Week 43 vs. Week 41	Pseudoneutralizing titers: Week 43 vs. Week 6	Pseudoneutralizing titers: Week 43 vs. Week 41
mRNA-1273	WA1 or D614G	NS	0.01	NS	<0.0001
	Delta	NS	0.003	NS	0.001
	Beta	0.05	0.006	0.022	0.001
	Omicron	0.041	0.003	0.049	0.005
mRNA-Omicron	WA1 or D614G	NS	0.001	NS	0.001
	Delta	NS	<0.0001	NS	<0.0001
	Beta	0.035	0.008	<0.0001	0.001
	Omicron	0.01	0.002	0.002	0.002

Figure 1. Kinetics of serum antibody responses following mRNA-1273 immunization and boost with mRNA-1273 or mRNA-Omicron

(A–F) Sera were collected at weeks 6, 40 or 41, and 43 post-immunization.

(A and B) IgG-binding titers to (A) variant S and (B) variant RBD expressed in AUC.

(C and D) Neutralizing titers to (C) live virus and (D) lentiviral pseudovirus expressed as the reciprocal ID_{50}.

(E) p values listed for week 43 titers compared with week 6 or 41 as indicated in Figures 1A–1D.

(legend continued on next page)

with GMT of 2 × 10^{12} and 2 × 10^{8} AUC for WA1 and Omicron, reflecting a 7-log decline for each strain. Similar antibody kinetics and hierarchy of potency were observed when measuring binding to the receptor binding domain (RBD) of the same variants, with titers to Omicron of 7 × 10^{11} AUC at week 6 and 8 × 10^{7} AUC at week 41 (Figure 1B). Nine months after the second dose of mRNA-1273 (week 41), NHP were boosted with 50 μg of homologous mRNA-1273 or heterologous virus challenge-matched mRNA-Omicron (n = 4/group) (Table S1). S-binding titers were restored to the same level as observed at week 6 following either a homologous or heterologous boost (Figure 1E), and titers to Omicron were still lower than all other variants.

Neutralizing antibody titers were then assessed using a live-virus assay (Figure 1C; Table S2). At week 6, neutralizing titers were highest to D614G followed by Delta, then Beta and Omicron. Titers to all variants markedly declined by week 41, including a drop in reciprocal 50% inhibitory dilution (ID_{50}) titers for D614G from 5,560 at week 6 to 330 at week 41 and for Omicron from 110 at week 6 to 33 at week 41. However, following either boost, neutralizing titers to D614G and Delta were increased similar to week 6 and titers to Beta and Omicron were greater than they had been at week 6 (Beta: p = 0.05 and 0.035; Omicron: p = 0.041 and 0.01 for mRNA-1273 and mRNA-Omicron, respectively) (Figure 1E). We substantiated these findings using a lentiviral pseudovirus neutralization assay similar to the one used to assess immune responses in human clinical trials (Figures 1D and 1E). Following either boost, pseudovirus neutralizing titers were greater to Beta and Omicron than they had been at the week 6 time point, including an increase in Omicron titers from 320 GMT to 2,980 GMT in the mRNA-1273 boost group and 1,930 GMT in the mRNA-Omicron boost group (Beta: p = 0.022 and < 0.0001; Omicron: p = 0.049 and 0.002 for mRNA-1273 and mRNA-Omicron, respectively). Further, titers to the two circulating sublineages of Omicron, BA.1 and BA.2, were comparable after either boost (Figure S1B).

The increase in neutralizing titers to all VOC tested after the third dose could suggest continued antibody maturation (Gaebler et al., 2021). To extend this analysis, we measured antibody avidity over time following immunization (Figure 1F). Serum antibody avidity to WA1 S-2P increased from a geometric mean avidity index of 0.43–0.61 from weeks 6 to 40, a comparable increase to our previous findings (Corbett et al., 2021a; Gagne et al., 2022). Similarly, avidity to Omicron S-2P rose from 0.44 to 0.67 (WA1 and Omicron S-2P: p < 0.0001). Following the boost, no further change was observed (p > 0.05).

Collectively, these data show that boosting with the homologous mRNA-1273 or mRNA-Omicron leads to comparable and significant increases in neutralizing antibody responses against all VOC including Omicron.

mRNA-1273 and mRNA-Omicron boosting increase mucosal antibody responses to Omicron

Upper and lower airway antibody responses are critical for mediating protection against SARS-CoV-2 and were assessed following immunization. Nasal washes (NW) and bronchoalveolar lavage fluid (BAL) were collected at weeks 8 (4 weeks after the initial mRNA-1273 immunizations), 39 (preboost), and 43 (2 weeks after the boost). At all time points, BAL and NW IgG S-binding titers followed the hierarchy of WA1 > Delta > Beta > Omicron (Figures 2A and 2B), the same trend detected in our serological assays. In BAL, immediately prior to the boost, GMT were 6.8 × 10^{6}, 4.0 × 10^{6}, 1.3 × 10^{6}, and 2.4 × 10^{4} AUC for WA1, Delta, Beta, and Omicron, respectively. These titers correlated with a 2-fold reduction for Delta compared with WA1, a 5-fold reduction for Beta, and a 280-fold reduction for Omicron. Following either boost, titers were increased by 3–4 logs for all variants. In NW, titers decreased from ~10^{11} for WA1, Delta, and Beta at week 8 to 1.3 × 10^{6}, 3.7 × 10^{5}, and 1.9 × 10^{5} at week 39 for WA1, Delta, and Beta, respectively. GMT to Omicron similarly declined from 8.8 × 10^{8} to 8.7 × 10^{3} AUC and were lower than WA1 and all other variants. Consistent with the findings in the BAL, either boost increased nasal antibody titers ~6–7 logs, with a GMT of ~10^{12} for WA1, Delta, and Beta and ~10^{10} for Omicron.

In a number of prior NHP studies, we have not been able to detect antibody neutralizing titers using pseudo- or live-virus assays from NW or BAL. However, based on its high sensitivity, we have used the angiotensin converting enzyme 2 receptor (ACE2) inhibition assay to measure antibody function as a surrogate for neutralization capacity (Corbett et al., 2021a; Gagne et al., 2022). Although the antigen for determination of binding titers was wild-type (WT) S, our ACE2 inhibition assay used stabilized S-2P (Table S3). In the BAL, 25%–50% median binding inhibition was observed for all variants at week 8, except for Omicron S-2P in which binding inhibition was low to undetectable (Figure 2C). ACE2 binding inhibition declined to a median of <15% for all variants by week 39. Following a boost with either mRNA-1273 or mRNA-Omicron, we observed greater ACE2 inhibition, although this increase did not reach significance due to the small number of animals in each group. Of note, although ACE2 inhibition of Omicron S-2P increased following the boost, it remained lower than all other variants. In the upper airway, ACE2 inhibition was low to undetectable at week 39 following the initial vaccine regimen for all variants. However, after either boost, there was an increase across all variants including Omicron to values higher than the initial peak at week 8 (Figure 2D). Thus, boosting with either vaccine was important for enhancing mucosal antibody binding and neutralization responses.

(F) Avidity index for WA1 S-2P- and Omicron S-2P-binding serum antibodies. p values for comparison of avidity index at weeks 6 versus 40 were identical for both boost cohorts.

Circles represent geometric means. Error bars represent geometric standard deviations. Assay limit of detection (LOD) indicated by dotted lines. Break in x-axis indicates a change in scale without a break in the range depicted. Responses to variants are color-coded as WA1 or D614G (black), Delta (blue), Beta (red), and Omicron (green). Arrows represent timepoints of immunizations. Following the boost at week 41, mRNA-1273-boosted NHP indicated by solid lines and mRNA-Omicron-boosted NHP indicated by dashed lines. 8 vaccinated NHP, split into 2 cohorts of 4 NHP postboost. See also Figure S1 for experimental schema and neutralizing responses to BA.2, Table S1 for mRNA-Omicron sequence, and Table S2 for detailed neutralizing titers.

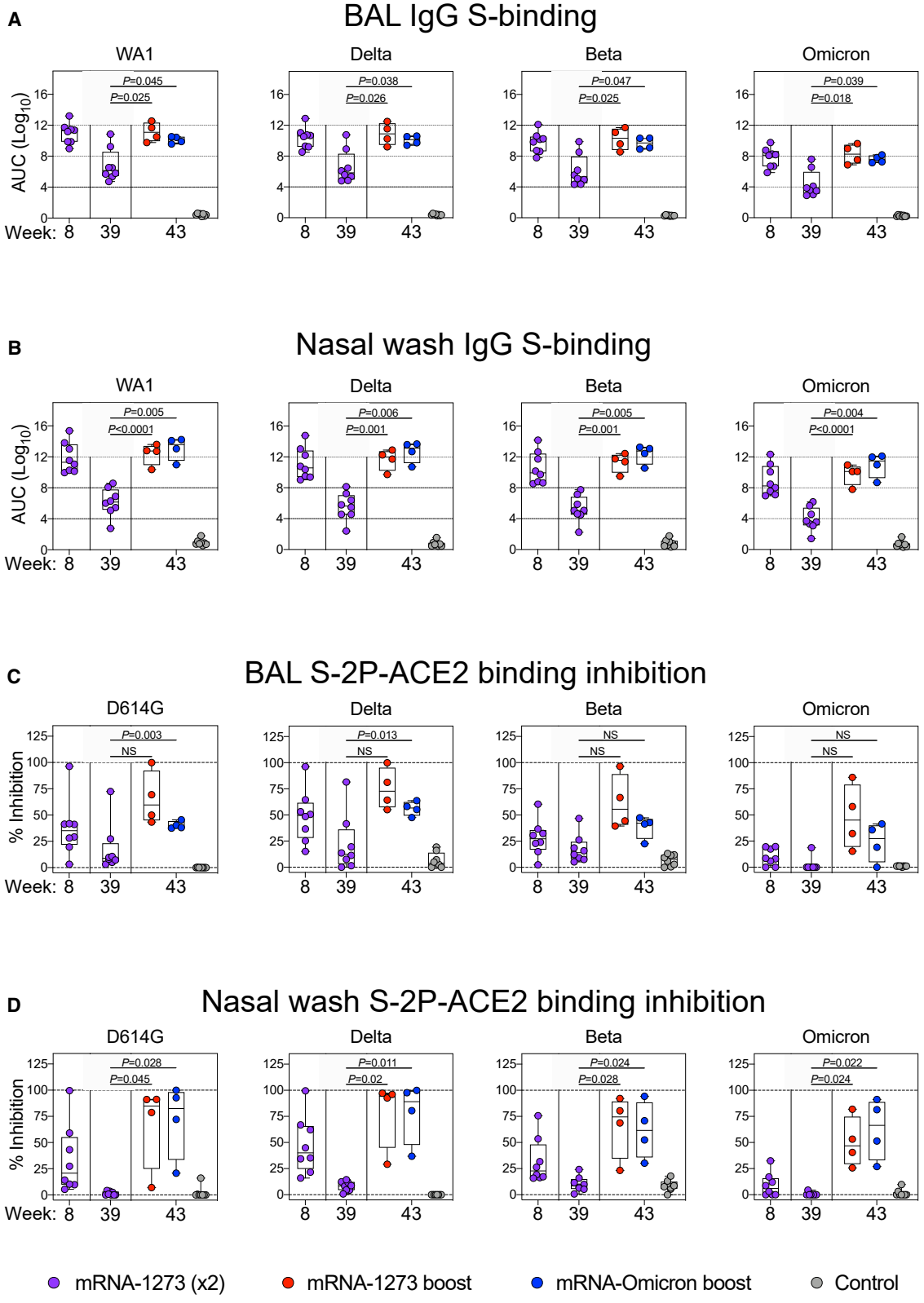

(legend on next page)

Similar expansion of cross-reactive S-2P-specific memory B cells following boosting

The observation of rapid and significant increases in binding and neutralizing antibody titers to Omicron in both blood and mucosal sites after homologous or heterologous mRNA boost suggests an anamnestic response involving the mobilization of cross-reactive memory B cells. Thus, we measured B cell binding to pairs of fluorochrome-labeled S-2P probes representing different VOC including Omicron at weeks 6, 41, and 43 (2 weeks postboost) (Figure S2).

Of the total S-2P specific memory B cell responses at week 6, 63% were dual specific and capable of binding both WA1 and Omicron probes, with 33% binding WA1 alone and only 4% which bound Omicron alone (Figures 3A and 4A). By week 41, the total S-specific memory B cell compartment in the blood had declined ~90% as a fraction of all class-switched memory B cells (Figure S3A), although the dual-specific population remained the largest fraction within the S-binding pool (Figure 4A).

Two weeks after boosting, there was an expansion of the total S-specific memory B cell compartment similar to that observed at week 6. Following an mRNA-1273 boost, 24% of all S-2P-specific memory B cells were specific for WA1 alone and 71% were dual specific for WA1 and Omicron. After the mRNA-Omicron boost, 81% were dual specific for WA1 and Omicron, with 12% specific for WA1 only (Figure 4A). Of note, we did not observe a population of Omicron-only memory B cells before or after the boost that was clearly distinct from background staining (Figure 3A). These data suggest a marked expansion of cross-reactive dual-specific WA1- and Omicron-positive B cells for either boost, with mRNA-1273 also expanding WA1-only B cell responses. The increase in cross-reactive B cells for WA1 and Omicron is consistent with the comparable and high-level of neutralizing titers against D614G and Omicron by either boost (Figures 1C and 1D). To extend these data, serologic mapping of antigenic sites on Omicron and WA1 RBD was performed. This analysis revealed that boosting with either mRNA-1273 or mRNA-Omicron elicited serum antibody reactivity with similar RBD specificities (Figure S4). Further, both boosts resulted in comparable antibody binding with the antigenic site defined by S309 (parent antibody of sotrovimab) that retains neutralizing capacity against the BA.1 sublineage of Omicron (VanBlargan et al., 2022).

To further explore the effect of boosting on anamnestic B cell responses, we phenotyped the activation status of S-binding memory B cells (Figure 4E). WA1 S-2P- and/or Omicron S-2P-binding memory B cells predominantly had an activated memory phenotype immediately after both the second and third doses.

Next, we determined the extent of cross-reactivity of B cells for two other VOC: Delta, which has recently cocirculated, and Beta, which shows significant neutralization resistance. Six weeks after vaccination, 68% of all Delta S-2P and/or Omicron S-2P memory B cells were dual specific and the remainder of S-binding memory B cells largely bound Delta alone (Figures 3B and 4B). Following a third dose, the frequency of dual-specific cells increased to 76% for mRNA-1273 and 85% for mRNA-Omicron, consistent with our findings on cross-reactive B cells using WA1 and Omicron S-2P probes.

We have previously reported that dual-specific WA1 S-2P and Delta S-2P memory B cells accounted for greater than 85% of all memory B cells that bound either spike after two immunizations with mRNA-1273 (Gagne et al., 2022). Here, we confirmed and extended these findings and show that after either boost, ~95% of all WA1- and/or Delta-binding memory B cells are dual-specific (Figures 3C and 4C). Similar findings were obtained with WA1 and Beta S-2P probes, in which the dual-specific population was 85% at week 6% and 90% following either boost (Figures 3D and 4D). Of note following the mRNA-Omicron boost, very few B cells were detected that only bound WA1 epitopes when costaining for Delta or Beta. Overall, the data show that cross-reactive cells were expanded following a boost with either mRNA-1273 or mRNA-Omicron, whereas only mRNA-1273 was capable of boosting memory B cells specific for WA1 alone (Figure S3).

Primary responses following variant-matched immunization

In addition to understanding how mRNA-1273 and mRNA-Omicron influenced immunity as a boost, it was also important to assess responses elicited by variant-matched vaccines used in a primary regimen. Thus, we immunized naive NHP with two doses of 100 μg mRNA-Omicron at weeks 0 and 4. Although a single dose of mRNA-Omicron in mRNA-1273-immunized NHP had failed to elicit a new population of memory B cells with unique specificities for Omicron S-2P (Figures 3A and 4A), primary immunization with mRNA-Omicron, in contrast, induced both WA1/Omicron cross-reactive memory B cells as well as B cells that bound only Omicron but not WA1 S-2P. Such responses were observed at 2 weeks after the prime and 2 weeks after the second dose of mRNA-Omicron although the kinetics of the response varied among animals (Figure S5A). Two weeks after either the first or second dose of mRNA-Omicron in naive animals, the magnitude of this response as measured by the frequency of total WA1- Omicron+ B cells was greater at a similar time after immunization than in the vaccinated NHP who had received mRNA-1273 prime and boost followed by the heterologous mRNA-Omicron boost (Figure S5B). These data highlight the differences between naive and vaccine-primed animals in

Figure 2. Kinetics of mucosal antibody responses following mRNA-1273 immunization and boost with mRNA-1273 or mRNA-Omicron

(A–D) BAL (A and C) and NW (B and D) were collected at weeks 8, 39, and 43 post-immunization.

(A and B) IgG-binding titers to WA1, Delta, Beta, and Omicron expressed in AUC.

(C and D) D614G, Delta, Beta, and Omicron S-2P-ACE2 binding inhibition in the presence of mucosal fluids. All samples diluted 1:5.

Circles indicate individual NHP. Boxes represent interquartile range with the median denoted by a horizontal line. Dotted lines are for visualization purposes and denote 4-$\log_{10}$ increases in binding titers (A and B) or 0% and 100% inhibition (C and D). Statistical analysis shown for week 43 responses compared with week 39 for both boost cohorts. In total, 8 controls and 8 vaccinated NHP, split into 2 cohorts postboost. See also Table S3 for list of amino acid replacements in variant-specific S-2P-ACE2 inhibition assays.

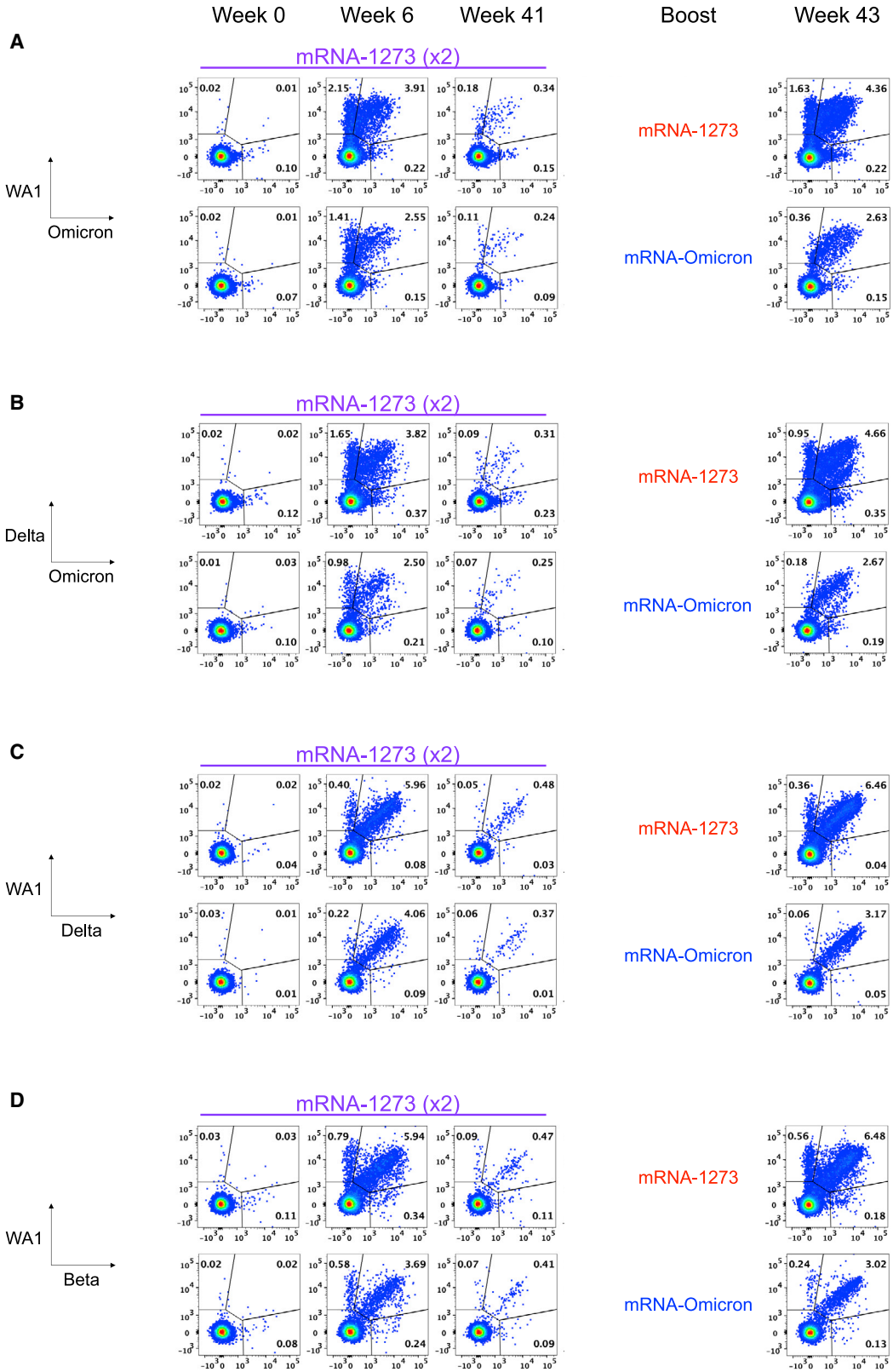

(legend on next page)

generating a population of memory B cells specific only for Omicron.

Further, recent studies in naive mice show that although vaccination with mRNA encoding WT or Delta S elicits neutralization that is cross-reactive to all the variants, vaccination with Omicron mRNA induces neutralization to Omicron only (Lee et al., 2022). Thus, we compared two-dose prime/boost regimens of mRNA-1273, mRNA-Omicron, and mRNA-Beta in naive NHP (Figure S6). Although vaccination with mRNA-1273 or mRNA-Beta elicited neutralizing responses to all variants tested, mRNA-Omicron elicited responses predominantly biased toward Omicron, with lower titers to the other variants. These data reveal a striking difference between using mRNA-Omicron as a boost to broadly enhance prior cross-reactive immunity compared with its use in a primary immunizing regimen.

S-2P-specific T cell responses in blood and BAL following vaccination

We have previously shown that mRNA-1273 immunization elicits T_H1, T_{FH}, and a low frequency of CD8 responses to S peptides in NHP and humans (Corbett et al., 2020, 2021a, 2021c; Gagne et al., 2022; Jackson et al., 2020). Consistent with the prior studies, we show that mRNA-1273 elicits T_H1, T_{FH}, and low-level CD8 T cell responses to WA1 S peptides at the peak of the response (week 6) that decline over time (Figures S7 and S8). Boosting with either mRNA-1273 or mRNA-Omicron increased T_{FH} responses that could be important for expanding the S-specific memory B cell population following the boost (Johnston et al., 2009; Nurieva et al., 2009; Tangye et al., 2002). T cell epitopes within Omicron S have been shown to be largely conserved (Choi et al., 2022); indeed, responses to Omicron-specific peptides after boosting were similar to those of WA1-specific peptides (Figure S9). Finally, we also detected T_H1 and CD8 T cells in BAL at week 8 that decreased to undetectable levels at week 39. Such responses were increased with either mRNA-1273 or mRNA-Omicron (Figure S8).

Boosting with mRNA-1273 or mRNA-Omicron provides equivalent protection in the lungs against Omicron challenge

To determine the extent of protection provided by a homologous mRNA-1273 or challenge virus-matched mRNA-Omicron boost following the two-dose mRNA-1273 immunization series, we obtained a new viral stock of Omicron, which was sequenced and confirmed to contain the canonical mutations present in the Omicron sublineage BA.1 (Figure S10).

Four weeks after administration of either boost, we challenged these NHP and 8 control NHP with 1×10^6 plaque forming units (PFU) via both intratracheal (IT) and intranasal (IN) routes (Figure S1A). The control NHP had previously been administered 50 μg of control mRNA formulated in lipid nanoparticles at the time of boost and had never been vaccinated.

BAL, nasal swabs (NS), and oral swabs (OS) were collected following challenge. Copy numbers of SARS-CoV-2 subgenomic RNA (sgRNA) were measured to determine the extent of viral replication. As sgRNA encoding for the N gene (sgRNA_N) are the most abundant transcripts produced due to the viral discontinuous transcription process (Kim et al., 2020), the sgRNA_N qRT-PCR assay was chosen for its enhanced sensitivity. On day 2 postinfection in the BAL, unvaccinated NHP had geometric mean copy numbers of 1×10^6 sgRNA_N per mL whereas the vaccinated NHP had 3×10^2 and 2×10^2 for the mRNA-1273 and mRNA-Omicron cohorts, respectively (Figure 5A). By day 4, all vaccinated NHP had undetectable levels of sgRNA_N, whereas copy numbers in the unvaccinated group had only declined to 3×10^5 per mL (either boost versus control on days 2 and 4: $p < 0.0001$).

In the nose, sgRNA_N copy numbers at days 1 to 4 were low for most animals and were not different between the control and vaccinated cohorts; hence protection following vaccination could not be determined (Figure 5B). At day 4, 5/8 controls had detectable virus in the nose as compared with 3/8 vaccinated NHP, with no clear difference between the boost cohorts. However, by day 8, 4/8 controls still had detectable sgRNA_N including 2 animals with increased copy numbers, whereas none of the vaccinated NHP had detectable sgRNA.

In assessing sgRNA_N in the throat, it is noteworthy that 2 days after challenge, only 1/8 vaccinated NHP (in either boost group) had detectable virus in the throat compared with 6/8 control NHP (Figure 5C).

We also measured the amount of culturable virus using a tissue culture infectious dose assay ($TCID_{50}$). No virus was detected in the BAL of any vaccinated NHP, whereas 8/8 and 7/8 control NHP had detectable virus 2 and 4 days after challenge, respectively (either boost versus control on day 2: $p < 0.0001$; day 4: $p = 0.0005$) (Figure 5D). In the NS, 1/8 boosted animals had culturable virus at any time point. In the unvaccinated control animals, 2/8 and 3/8 NHP had culturable virus in the nose 2 and 4 days after challenge, respectively (Figure 5E).

Virus antigen and pathology in the lungs after challenge

To assess lung pathology in NHP, 2 of the animals in each group were euthanized on day 8 following Omicron challenge, and the amount of virus antigen (SARS-CoV-2 N) and inflammation in the lungs were assessed (Figure 6). N antigen was detected in variable amounts in the lungs of both control animals. When present, virus antigen was often associated with the alveolar capillaries and, occasionally, nearby immune cells. There was no evidence of virus antigen in the lungs of the vaccinated NHP.

Animals from both boost groups displayed histopathologic alterations that were classified as minimal to mild or moderate. Inflammation was largely characterized by mild and patchy expansion of alveolar capillaries, generalized alveolar capillary hypercellularity, mild and regional type II pneumocyte

Figure 3. Memory B cell specificities following immunization and boosting

(A–D) Representative flow cytometry plots showing single variant-specific (top left and bottom right quadrant) and dual-variant-specific (top right quadrant) memory B cells at weeks 0, 6, 41, and 43 post-immunization. Event frequencies per gate are expressed as a percentage of all class-switched memory B cells. Cross-reactivity shown for (A) WA1 and Omicron S-2P, (B) Delta and Omicron S-2P, (C) WA1 and Delta S-2P, and (D) WA1 and Beta S-2P. See also Figure S2 for B cell-gating strategy.

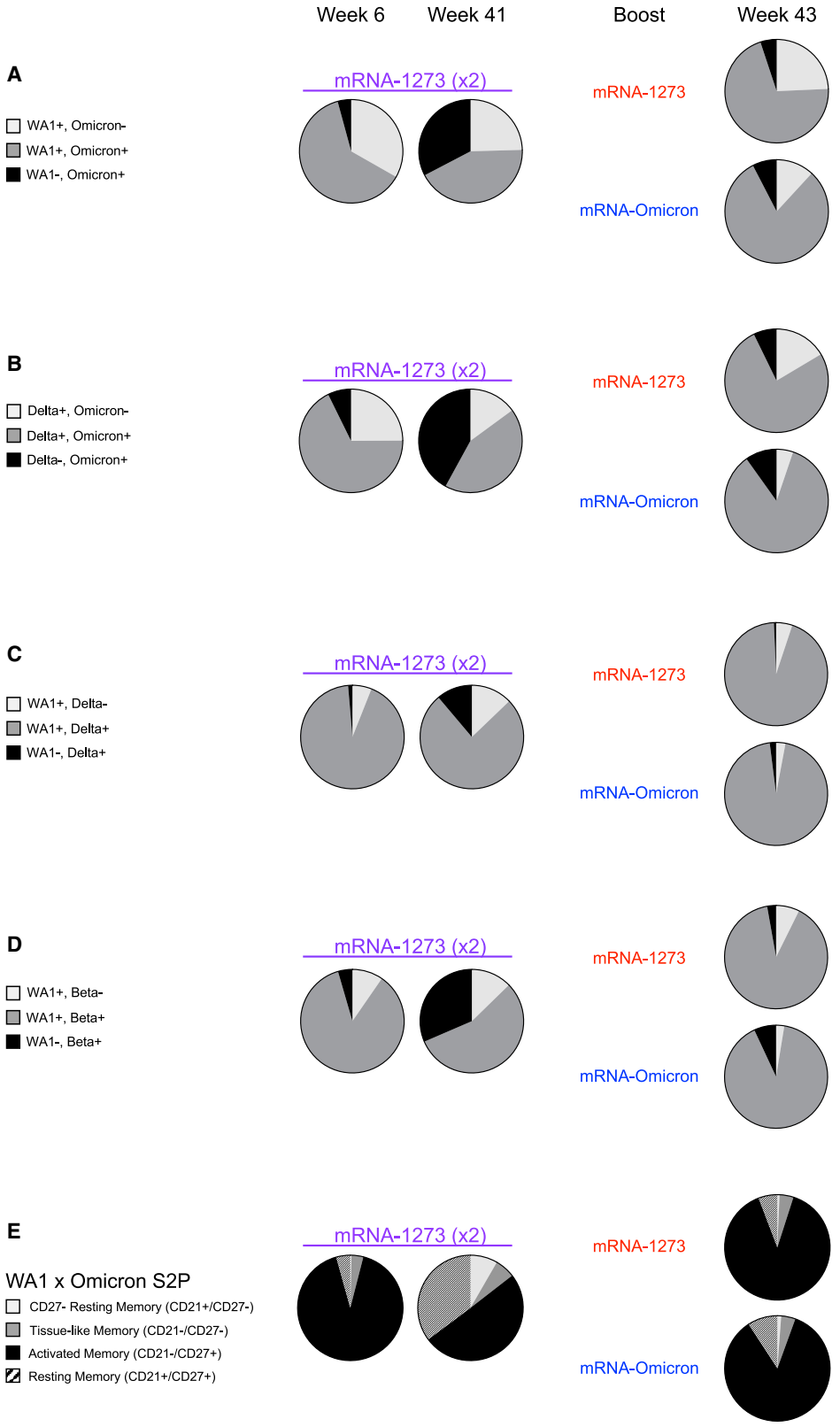

(legend on next page)

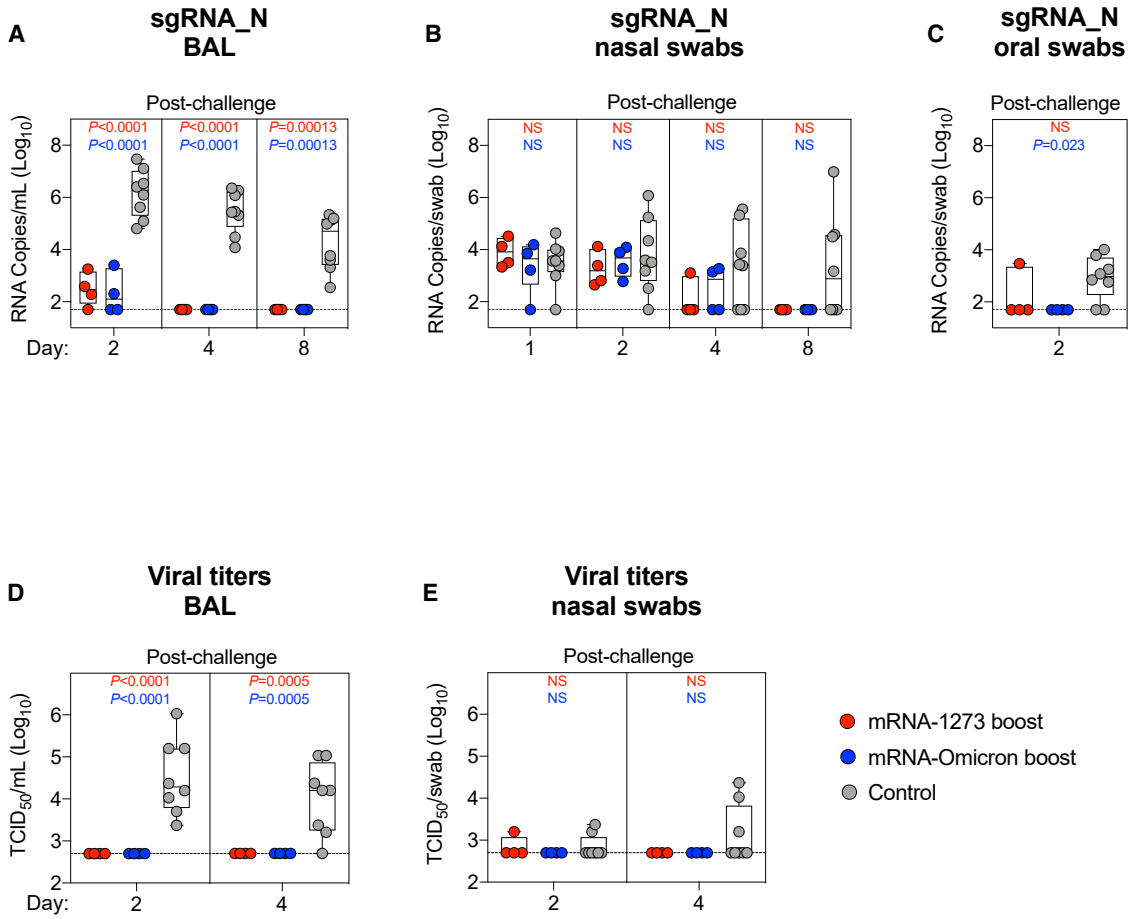

Figure 5. Boosting with ancestral or Omicron-matched vaccine provides equivalent protection in the lungs against Omicron challenge

(A–E) BAL (A and D), NS (B and E), and OS (C) were collected at the indicated times following challenge with 1 × 10^6 PFU Omicron.

(A–C) Omicron sgRNA_N copy numbers per mL of BAL (A) or per swab (B and C).

(D and E) Viral titers per mL of BAL (D) or per swab (E).

Circles indicate individual NHP. Boxes represent interquartile range with the median denoted by a horizontal line. Assay LOD indicated by dotted lines. Statistical analysis shown for cohorts boosted with mRNA-1273 (red text) or mRNA-Omicron (blue text) in comparison with controls at each timepoint. 8 controls and 4 vaccinated NHP per boost cohort. See also Figure S10 for Omicron challenge stock sequence.

hyperplasia and, less frequently, scattered collections of immune cells within some alveolar spaces. In contrast, unvaccinated animals were characterized as having a moderate-to-severe pathology. Lung sections from controls included features characterized by moderate and often diffuse alveolar capillary expansion, diffuse hypercellularity, moderate type II pneumocyte hyperplasia and multiple areas of perivascular cellular infiltration. Together, these data indicate that protection against Omicron was robust in the lungs regardless of boost selection.

DISCUSSION

Omicron has become the dominant global variant of SARS-CoV-2 due to its transmission advantage relative to Delta and

Figure 4. Similar expansion of cross-reactive S-2P-specific memory B cells following boost with mRNA-1273 or mRNA-Omicron

(A–D) Pie charts indicating the proportion of total S-binding memory B cells that are cross-reactive (dark gray) or specific for the indicated variants (black or light gray) for all NHP (geomean) at weeks 6, 41, and 43 post-immunization. Where applicable, memory B cells specific only for WA1 or Delta are represented by the light gray segment. Cross-reactivity shown for (A) WA1 and Omicron S-2P, (B) Delta and Omicron S-2P, (C) WA1 and Delta S-2P, and (D) WA1 and Beta S-2P. 4–7 NHP per group.

(E) Pie charts indicating the proportion of total S-2P-binding memory B cells (geomean) that have a phenotype consistent with resting memory (pattern), activated memory (black), tissue-like memory (dark gray), or CD27-negative resting memory (light gray) B cells at weeks 6, 41, and 43 post-immunization. Analysis shown here for memory B cells that bind to WA1 and/or Omicron S-2P. 4–7 NHP per group.

See also Figure S3 for frequencies of cross-reactive S-2P memory B cells, Figure S4 for serum epitope reactivity, Figures S5 and S6 for primary responses after variant-matched vaccination in naive NHP, and Figures S7, S8, and S9 for T cell responses after boosting.

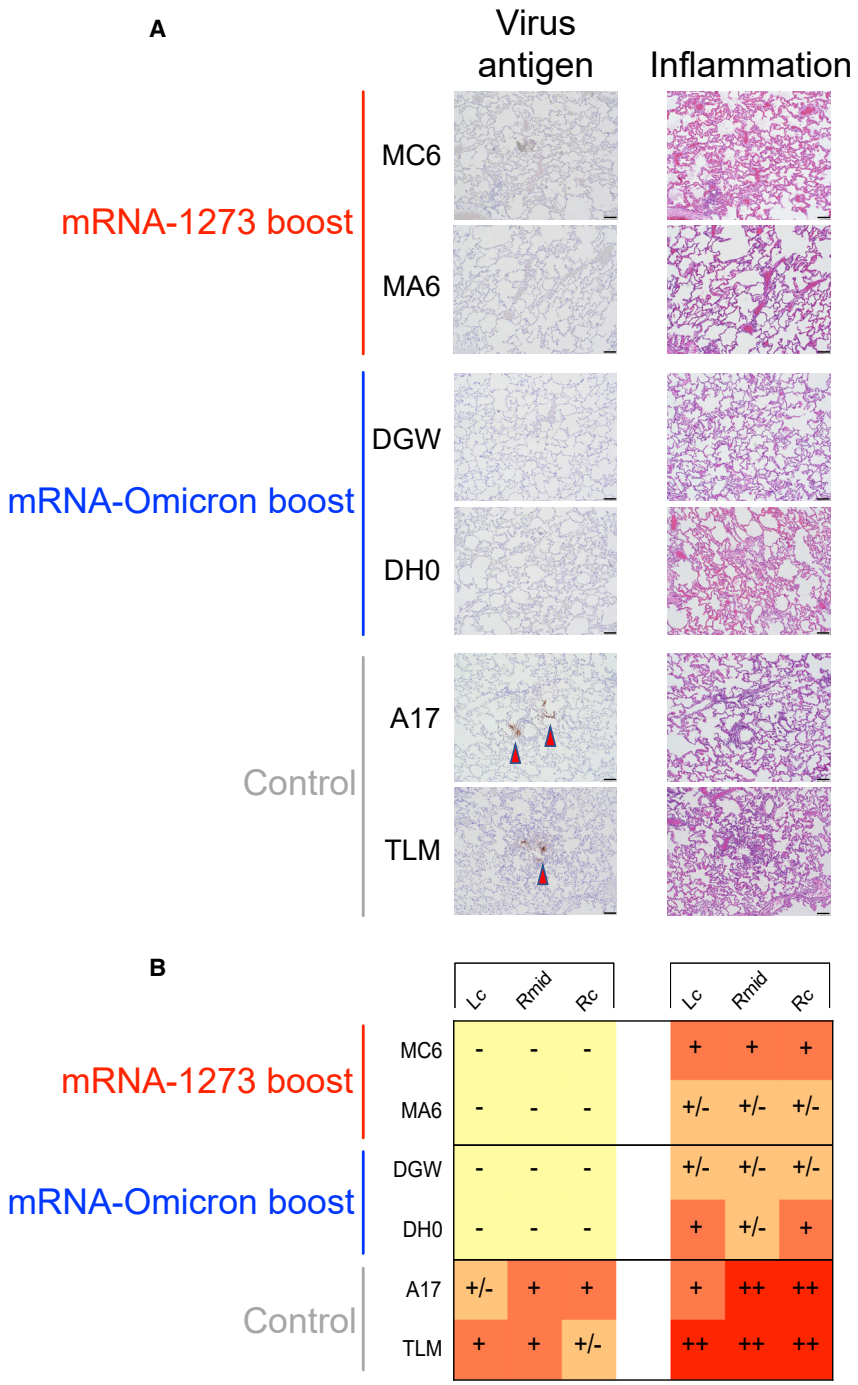

Figure 6. Virus antigen and pathology in the lungs after challenge

(A and B) 2 NHP per group were euthanized on day 8 postchallenge and tissue sections taken from lungs. (A) Left: representative images indicating detection of SARS-CoV-2 N antigen by immunohistochemistry with a polyclonal anti-N antibody. Antigen-positive foci are marked by a red arrow. Right: hematoxylin and eosin stain (H&E) illustrating the extent of inflammation and cellular infiltrates. Images at 10× magnification with black bars for scale (100 μm).

(B) SARS-CoV-2 antigen and inflammation scores in the left cranial lobe (Lc), right middle lobe (Rmid), and right caudal lobe (Rc) of the lungs. Antigen scoring legend: – no antigen detected; +/– rare to occasional foci; + occasional to multiple foci; ++ multiple to numerous foci; +++ numerous foci. Inflammation scoring legend: – absent to minimal inflammation; +/– minimal to mild inflammation; + mild to moderate inflammation; ++ moderate-to-severe inflammation; +++ severe inflammation. Horizontal rows correspond to individual NHP depicted above (A).

its ability to evade prior immunity (Grabowski et al., 2022; Viana et al., 2022). Vaccine efficacy against infection with Omicron has declined, and boosting with a third dose of an mRNA COVID-19 vaccine matched to the prototype strain has been shown to restore immunity and protection (Accorsi et al., 2022; Garcia-Beltran et al., 2022; Hansen et al., 2021; Pajon et al., 2022; Tseng et al., 2022). Here, we immunized NHP with 2 doses of mRNA-1273 (100 μg) and boosted them ~9 months later with 50 μg of either mRNA-1273 or mRNA-Omicron prior to challenge with Omicron virus. The principal findings were as follows: (1) 9 months after the two-dose regimen, neutralizing and binding antibody titers to Omicron had declined substantially in blood and mucosal airways; (2) after the boost, neutralizing antibody titers to ancestral strains were restored and those to Omicron were increased compared with the peak response after the initial prime and boost; (3) both boosts expanded cross-reactive memory B cells but only the homologous boost was capable of expanding B cells specific for epitopes unique to the ancestral strain; and (4) both boosts provided complete protection in the lungs and limited protection in the upper airway after Omicron challenge.

Following either mRNA-1273 or mRNA-Omicron boost, there was essentially complete protection in the lower airway with no culturable virus by day 2 and no detectable sgRNA_N by day 4. These data are comparable with our previous findings of equivalent upper and lower airway protection following Beta challenge 2 months after boosting mRNA-1273-immunized NHP with either mRNA-1273 or mRNA-Beta (Corbett et al., 2021a). In contrast to the lower airway, there were no clear and consistent differences in sgRNA_N copy number at days 2 or 4 in the upper airway of vaccinated or control NHP. Of note, more of the control animals had detectable sgRNA at day 4 and increased sgRNA at day 8 as compared with the boosted animals. We would also note that the amount of Omicron replication as assessed by sgRNA or

culturable virus in the control animals is demonstrably different than in our prior studies in which NHP were challenged with WA1, Delta, or Beta (Corbett et al., 2020, 2021c; Gagne et al., 2022). These findings are consistent with evidence for reduced overall severity of Omicron infection in animal models of COVID-19 compared with other variants (Bentley et al., 2021; Halfmann et al., 2022; Suryawanshi et al., 2022). Overall, the findings here of high-level protection in the lungs recapitulate observations in vaccinated humans of reduced disease severity following infection with Omicron (Abdullah et al., 2022; Sigal, 2022; Wolter et al., 2022). Our data also complement recent findings on protection from Omicron infection in hamsters immunized with replicating RNA matched to the ancestral strain or Omicron S (Hawman et al., 2022).

Neutralizing antibodies to Omicron in the blood or ACE2 binding inhibitory antibodies in the airway mucosa were low after the first 2 doses of mRNA-1273 at weeks 6–8 and low to undetectable ~9 months later. Importantly, either mRNA-1273 or mRNA-Omicron boosts were able to significantly increase neutralizing antibody titers against Omicron and Beta beyond their initial peak consistent with a rapid recall B cell response. This also implies that neutralizing antibody titers at extended times after vaccination may not be a reliable surrogate either for vaccine efficacy in the lower airway or for predicting responses following a boost or infection as they may not reflect the recall capacity of the underlying memory B cell population.

The observation that boosting with either mRNA-1273 or mRNA-Omicron resulted in the expansion of a similarly high frequency of cross-reactive B cells likely stems from the recall of prior immune memory after a related antigenic encounter. This principle has been termed original antigenic sin, imprinting, and back boosting (Fonville et al., 2014; Francis, 1960; Köhler et al., 1994). Recall of prior immunity may be deleterious or beneficial as exemplified by the impact of the circulating influenza A subtypes at the time of an individual's first exposure after birth on patterns of disease susceptibility to subsequent pandemic influenza A outbreaks (Gostic et al., 2016; Worobey et al., 2014). The current worldwide distribution and evolution of SARS-CoV-2, however, is quite different from that of influenza A. Although multiple subtypes of influenza A circulate with different levels of co-dominance, SARS-CoV-2 distribution has generally become rapidly dominated by a single variant—currently Omicron—before replacement by another that, for various reasons, is more transmissible. The question therefore is whether there is added value from boosting with a heterologous vaccine matched to the dominant circulating variant or whether cross-reactive B cell recall immunity elicited by boosting with the original vaccine is sufficient to reduce infection and disease severity. As we have now shown in two different NHP studies, boosting animals with either mRNA-Beta (Corbett et al., 2021a) or mRNA-Omicron has not yet been shown to provide any significant advantage over mRNA-1273 in recalling high titer neutralizing antibodies across all variants tested in the short term and protecting from virus replication after challenge. These considerations may apply to the large numbers of individuals with prior immunity from vaccination or infection with current and previous variants. Importantly, the conclusions related to postboost immunity are limited to the short duration of immune assessment in our studies. It is conceivable that mobilization of pre-existing memory B cells may dominate the initial immune response to a booster dose and that further longitudinal analysis could reveal B cell populations with new specificities to the matched variant boost (Sokal et al., 2021).

Looking to the future, however, if Omicron, or a closely antigenically related variant, remains the dominant circulating variant for some years to come, then it is possible that a change in the initial vaccine regimen would be warranted, particularly in immunologically naive populations such as children as they reach the age of eligibility for approved COVID-19 vaccines. Importantly, it would need to be established that a switch in COVID-19 vaccine design to match the current dominant variant would not limit responses against variants that may be antigenically distant from Omicron but close to the prototype. In fact, we show that in naive animals, mRNA-Omicron as an initial prime and boost regimen skewed neutralizing responses predominantly toward Omicron with more limited neutralization against past variants, consistent with recent data from primary Omicron infection in humans (Richardson et al., 2022; Rössler et al., 2022). Thus, a combination or bivalent vaccine to generate B cells specific for the current variant as well as cross-reactive to other variants might ensure greater breadth of neutralization in naive hosts (Lee et al., 2022).

In summary, our findings highlight two important factors that will impact management of this pandemic. The first is the design of the vaccine and whether it should be changed based on the currently circulating variant. At present, boosting previously vaccinated NHP and humans with mRNA-1273 provides significant increases in neutralizing antibodies and is sufficient to prevent severe disease after exposure from all known variants (Accorsi et al., 2022; Andrews et al., 2022; Choi et al., 2021; Corbett et al., 2021a; Garcia-Beltran et al., 2022; Pajon et al., 2022; Tseng et al., 2022). Variant-matched vaccines might be preferable if additional clinical studies showed a significant benefit in neutralization or protection against new emergent variants that were even further antigenically distant such that there was limited boosting of cross-reactive B cells. Such a change in vaccine design would likely have a greater impact on eliciting variant-specific responses in immunologically naive individuals who are unencumbered by prior immune memory. Second, as neutralizing antibody titers wane with time after vaccination, their ability to serve as a surrogate for vaccine efficacy or to predict clinical outcomes against severe disease after infection with VOC may become diminished. Thus, the determination of when to administer a boost may depend on the recall capacity of the underlying memory B cell population. These considerations will become clear as human clinical data are made available.

Limitations of the study

There are several limitations to this study. First, NHP models may not fully recapitulate clinical data in humans regarding the extent of virus replication necessary for the enhanced transmission of Omicron compared with prior variants. Here, viral titers were low in the lungs and low to undetectable in the upper airway. Second, neutralizing antibody titers in NHP are 5- to 10-fold greater than in humans who received the same dose and

regimen of mRNA-1273 with a boost (Edara et al., 2022; Pajon et al., 2022). Third, we only assessed immune responses 2 weeks postboost since animals were challenged shortly thereafter. It is possible that there may be differences in the durability of neutralizing responses following an Omicron boost. Moreover, as half of the animals in each boost cohort were euthanized 8 days after challenge, we did not have a sufficient number of animals to determine the kinetics of postchallenge immune responses. Fourth, it is also possible that a second dose of mRNA-Omicron in mRNA-1273-vaccinated animals, or a further boost after Omicron challenge, may elicit a population of B cells with greater neutralization toward Omicron. In addition, we did not assess a bivalent boost of mRNA-1273 and mRNA-Omicron which might elicit higher neutralizing responses than either alone. Finally, since we sought to compare two different mRNA boosts, we did not have an unboosted group to determine whether the boost enhanced protection. As all the boosted NHP were completely protected in the lungs, we were unable to determine an immune threshold for protection.

STAR★METHODS

Detailed methods are provided in the online version of this paper and include the following:

- KEY RESOURCES TABLE
- RESOURCE AVAILABILITY
  - Lead contact
  - Materials availability
  - Data and code availability
- EXPERIMENTAL MODEL AND SUBJECT DETAILS
  - Preclinical mRNA and lipid nanoparticles
  - Rhesus macaque model and immunizations
- METHOD DETAILS
  - Cells and viruses
  - Sequencing of Omicron virus stock
  - Omicron challenge
  - Serum and mucosal antibody titers
  - S-2P antigens
  - S-2P-ACE2 binding inhibition
  - Focus reduction neutralization assay
  - Lentiviral pseudovirus neutralization
  - Serum antibody avidity
  - Epitope mapping
  - B cell probe binding
  - Intracellular cytokine staining
  - Subgenomic RNA quantification
  - N gene
  - $TCID_{50}$ assay
  - Histopathology and immunohistochemistry
- QUANTIFICATION AND STATISTICAL ANALYSIS

SUPPLEMENTAL INFORMATION

Supplemental information can be found online at https://doi.org/10.1016/j.cell.2022.03.038.

ACKNOWLEDGMENTS

We would like to thank G. Alvarado for experimental organization and administrative support. Ethan Tyler designed the graphical abstract. The VRC Production Program (VPP) provided the WA1 protein for the avidity assay. VPP contributors include C. Anderson, V. Bhagat, J. Burd, J. Cai, K. Carlton, W. Chuenchor, N. Clbelli, G. Dobrescu, M. Figur, J. Gall, H. Geng, D. Gowetski, K. Gulla, L. Hogan, V. Ivleva, S. Khayat, P. Lei, Y. Li, I. Loukinov, M. Mai, S. Nugent, M. Pratt, E. Reilly, E. Rosales-Zavala, E. Scheideman, A. Shaddeau, A. Thomas, S. Upadhyay, K. Vickery, A. Vinitsky, C. Wang, C. Webber, and Y. Yang. This project has been funded in part by both the Intramural Program of the National Institute of Allergy and Infectious Diseases, National Institutes of Health, Department of Health and Human Services and under HHSN272201400004C (NIAID Centers of Excellence for Influenza Research and Surveillance, CEIRS) and NIH P51 OD011132 awarded to Emory University. This work was also supported in part by the Emory Executive Vice President for Health Affairs Synergy Fund award, COVID-Catalyst-I3 Funds from the Woodruff Health Sciences Center and Emory School of Medicine, the Pediatric Research Alliance Center for Childhood Infections and Vaccines and Children's Healthcare of Atlanta, and Woodruff Health Sciences Center 2020 COVID-19 CURE Award.

AUTHOR CONTRIBUTIONS

M.R., N.J.S., D.C.D., and R.A.S. designed experiments. M.G., J.I.M., K.E.F., S.F.A., B.J.F., A.P.W., D.A.W., B.C.L., C.M., N.J.-B., R.C., S.L.F., M.P., M.E., V.-V.E., N.V.M., M.M., L.M., C.C.H., B.M.N., K.W.B., C.N.M.D., J.C., D.R.F., J.-P.M.T., E.M., L.P., A.V.R., B.N., D.V., A. Cook, A.D., K.S., S.T.N., S.G., A.R.H., F.L., J.R.-T., C.G.L., S.A., M.G.L., H.A., K.S.C., M.C.N., A.B.M., M.S.S., I.N.M., M.R., N.J.S., D.C.D., and R.A.S. performed, analyzed, and/or supervised experiments. M.G., J.I.M., K.E.F., S.F.A., D.A.W., I.N.M., and D.C.D. designed figures. I.-T.T., J.T., M.N., M.B., J.W., L.W., W.S., N.A.D.-R., Y.Z., E.S.Y., K.L., S.O., S.D.S., A.S.O., C.L., D.R.H., G.-Y.C., G.S.-J., I.R., Y.-T.L., A.M., K.W., J.R.M., A. Carfi, P.D.K., and D.K.E. provided critical reagents. M.G., J.I.M., D.C.D., and R.A.S. wrote manuscript. All authors edited the manuscript and provided feedback on research.

DECLARATION OF INTERESTS

K.S.C. is an inventor on U.S. Patent no. 10,960,070 B2 and International Patent Application no. WO/2018/081318 entitled "Prefusion Coronavirus Spike Proteins and Their Use." K.S.C. is an inventor on U.S. Patent Application no. 62/972,886 entitled "2019-nCoV Vaccine." A.R.H., L.W., W.S., Y.Z., E.S.Y., J.R.M., P.D.K., M.R., N.J.S., and D.C.D. are inventors on U.S. Patent Application no. 63/147,419 entitled "Antibodies Targeting the Spike Protein of Coronaviruses." L.P., A.V.R., B.N., D.V., A. Cook, A.D., K.S., H.A., and M.G.L. are employees of Bioqual. K.S.C., L.W., W.S., and Y.Z. are inventors on multiple U.S. Patent Applications entitled "Anti-Coronavirus Antibodies and Methods of Use." G.-Y.C., G.S.-J., I.R., Y.-T.L., A.M., K.W., A. Carfi, and D.K.E. are employees of Moderna. M.S.S. serves on the scientific board of advisors for Moderna and Ocugen. The other authors declare no competing interests.

Received: February 19, 2022
Revised: March 11, 2022
Accepted: March 23, 2022
Published: March 25, 2022

REFERENCES

Abdullah, F., Myers, J., Basu, D., Tintinger, G., Ueckermann, V., Mathebula, M., Ramlall, R., Spoor, S., de Villiers, T., Van der Walt, Z., et al. (2022). Decreased severity of disease during the first global omicron variant covid-19 outbreak in a large hospital in tshwane, South Africa. Int. J. Infect. Dis. *116*, 38–42.

Accorsi, E.K., Britton, A., Fleming-Dutra, K.E., Smith, Z.R., Shang, N., Derado, G., Miller, J., Schrag, S.J., and Verani, J.R. (2022). Association between 3

doses of mRNA COVID-19 vaccine and symptomatic infection caused by the SARS-CoV-2 omicron and Delta variants. JAMA *327*, 639–651.

Andrews, N., Stowe, J., Kirsebom, F., Toffa, S., Sachdeva, R., Gower, C., Ramsay, M., and Lopez Bernal, J.L. (2022). Effectiveness of COVID-19 booster vaccines against covid-19-related symptoms, hospitalisation and death in England. Nat. Med. Published online January *14*, 2022. https://doi.org/10.1038/s41591-022-01699-1.

Baden, L.R., El Sahly, H.M., Essink, B., Follmann, D., Neuzil, K.M., August, A., Clouting, H., Fortier, G., Deng, W., and Han, S. (2021a). Phase 3 Trial of mRNA-1273 during the Delta-Variant Surge. N Engl J Med *385*, 2485–2487.

Baden, L.R., El Sahly, H.M., Essink, B., Kotloff, K., Frey, S., Novak, R., Diemert, D., Spector, S.A., Rouphael, N., Creech, C.B., et al.; COVE Study Group (2021b). Efficacy and Safety of the mRNA-1273 SARS-CoV-2 Vaccine. N Engl J Med *384*, 403–416.

Barda, N., Dagan, N., Cohen, C., Hernán, M.A., Lipsitch, M., Kohane, I.S., Reis, B.Y., and Balicer, R.D. (2021). Effectiveness of a third dose of the BNT162b2 mRNA COVID-19 vaccine for preventing severe outcomes in Israel: an observational study. Lancet *398*, 2093–2100.

Bar-On, Y.M., Goldberg, Y., Mandel, M., Bodenheimer, O., Freedman, L., Alroy-Preis, S., Ash, N., Huppert, A., and Milo, R. (2021). Protection against Covid-19 by BNT162b2 booster across age groups. N. Engl. J. Med. *385*, 2421–2430.

Bentley, E.G., Kirby, A., Sharma, P., Kipar, A., Mega, D.F., Bramwell, C., Penrice-Randal, R., Prince, T., Brown, J.C., Zhou, J., et al. (2021). SARS-CoV-2 Omicron-B.1.1.529 Variant leads to less severe disease than Pango B and Delta variants strains in a mouse model of severe COVID-19. Preprint at bioRxiv, 2021.2012.2026.474085.

Bergwerk, M., Gonen, T., Lustig, Y., Amit, S., Lipsitch, M., Cohen, C., Mandelboim, M., Levin, E.G., Rubin, C., Indenbaum, V., et al. (2021). Covid-19 breakthrough infections in vaccinated health care workers. N. Engl. J. Med. *385*, 1474–1484.

Cele, S., Jackson, L., Khoury, D.S., Khan, K., Moyo-Gwete, T., Tegally, H., San, J.E., Cromer, D., Scheepers, C., Amoako, D.G., et al. (2022). Omicron extensively but incompletely escapes Pfizer BNT162b2 neutralization. Nature *602*, 654–656.

Choi, A., Koch, M., Wu, K., Chu, L., Ma, L., Hill, A., Nunna, N., Huang, W., Oestreicher, J., Colpitts, T., et al. (2021). Safety and immunogenicity of SARS-CoV-2 variant mRNA vaccine boosters in healthy adults: an interim analysis. Nat. Med. *27*, 2025–2031.

Choi, S.J., Kim, D.U., Noh, J.Y., Kim, S., Park, S.H., Jeong, H.W., and Shin, E.C. (2022). T cell epitopes in SARS-CoV-2 proteins are substantially conserved in the Omicron variant. Cell. Mol. Immunol. *19*, 447–448.

Corbett, K.S., Flynn, B., Foulds, K.E., Francica, J.R., Boyoglu-Barnum, S., Werner, A.P., Flach, B., O'Connell, S., Bock, K.W., Minai, M., et al. (2020). Evaluation of the mRNA-1273 vaccine against SARS-CoV-2 in nonhuman primates. N. Engl. J. Med. *383*, 1544–1555.

Corbett, K.S., Gagne, M., Wagner, D.A., O'Conell, S., Narpala, S.R., Flebbe, D.R., Andrew, S.F., Davis, R.L., Flynn, B., et al. (2021a). Protection against SARS-CoV-2 beta variant in mRNA-1273 vaccine-boosted nonhuman primates. Science *374*, eabl8912.

Corbett, K.S., Nason, M.C., Flach, B., Gagne, M., O'Connell, S., Johnston, T.S., Shah, S.N., Edara, V.V., Floyd, K., Lai, L., et al. (2021b). Immune correlates of protection by mRNA-1273 vaccine against SARS-CoV-2 in nonhuman primates. Science *373*, eabj0299.

Corbett, K.S., Werner, A.P., Connell, S.O., Gagne, M., Lai, L., Moliva, J.I., Flynn, B., Choi, A., Koch, M., Foulds, K.E., et al. (2021c). mRNA-1273 protects against SARS-CoV-2 beta infection in nonhuman primates. Nat. Immunol. *22*, 1306–1315.

Dagan, N., Barda, N., Kepten, E., Miron, O., Perchik, S., Katz, M.A., Hernán, M.A., Lipsitch, M., Reis, B., and Balicer, R.D. (2021). BNT162b2 mRNA Covid-19 vaccine in a nationwide mass vaccination setting. N. Engl. J. Med. *384*, 1412–1423.

Davies, M.-A., Kassanjee, R., Rousseau, P., Morden, E., Johnson, L., Solomon, W., Hsiao, N.-Y., Hussey, H., Meintjes, G., Paleker, M., et al. (2022). Outcomes of laboratory-confirmed SARS-CoV-2 infection in the Omicron-driven fourth wave compared with previous waves in the Western Cape Province, South Africa. Preprint at medRxiv, 2022.2001.2012.22269148.

DiPiazza, A.T., Leist, S.R., Abiona, O.M., Moliva, J.I., Werner, A., Minai, M., Nagata, B.M., Bock, K.W., Phung, E., Schäfer, A., et al. (2021). COVID-19 vaccine mRNA-1273 elicits a protective immune profile in mice that is not associated with vaccine-enhanced disease upon SARS-CoV-2 challenge. Immunity *54*, 1869–1882.e6.

Donaldson, M.M., Kao, S.F., and Foulds, K.E. (2019). OMIP-052: an 18-color panel for measuring Th1, Th2, Th17, and Tfh responses in rhesus macaques. Cytometry A *95*, 261–263.

Edara, V.V., Manning, K.E., Ellis, M., Lai, L., Moore, K.M., Foster, S.L., Floyd, K., Davis-Gardner, M.E., Mantus, G., Nyhoff, L.E., et al. (2022). mRNA-1273 and BNT162b2 mRNA vaccines have reduced neutralizing activity against the SARS-CoV-2 omicron variant. Cell Rep. Med. *3*, 100529.

Edara, V.V., Norwood, C., Floyd, K., Lai, L., Davis-Gardner, M.E., Hudson, W.H., Mantus, G., Nyhoff, L.E., Adelman, M.W., Fineman, R., et al. (2021a). Infection- and vaccine-induced antibody binding and neutralization of the B.1.351 SARS-CoV-2 variant. Cell Host Microbe *29*, 516–521.e3.

Edara, V.V., Pinsky, B.A., Suthar, M.S., Lai, L., Davis-Gardner, M.E., Floyd, K., Flowers, M.W., Wrammert, J., Hussaini, L., Ciric, C.R., et al. (2021b). Infection and vaccine-induced neutralizing-antibody responses to the SARS-CoV-2 B.1.617 Variants. N. Engl. J. Med. *385*, 664–666.

Fonville, J.M., Wilks, S.H., James, S.L., Fox, A., Ventresca, M., Aban, M., Xue, L., Jones, T.C., Le, N.M.H., Pham, Q.T., et al. (2014). Antibody landscapes after influenza virus infection or vaccination. Science *346*, 996–1000.

Francica, J.R., Flynn, B.J., Foulds, K.E., Noe, A.T., Werner, A.P., Moore, I.N., Gagne, M., Johnston, T.S., Tucker, C., Davis, R.L., et al. (2021). Protective antibodies elicited by SARS-CoV-2 spike protein vaccination are boosted in the lung after challenge in nonhuman primates. Sci. Transl. Med. *13*, eabi4547.

Francis, T. (1960). On the doctrine of original antigenic sin. Proc. Am. Philos. Soc. *104*, 572–578.

Gaebler, C., Wang, Z., Lorenzi, J.C.C., Muecksch, F., Finkin, S., Tokuyama, M., Cho, A., Jankovic, M., Schaefer-Babajew, D., Oliveira, T.Y., et al. (2021). Evolution of antibody immunity to SARS-CoV-2. Nature *591*, 639–644.

Gagne, M., Corbett, K.S., Flynn, B.J., Foulds, K.E., Wagner, D.A., Andrew, S.F., Todd, J.M., Honeycutt, C.C., McCormick, L., Nurmukhambetova, S.T., et al. (2022). Protection from SARS-CoV-2 Delta one year after mRNA-1273 vaccination in rhesus macaques coincides with anamnestic antibody response in the lung. Cell *185*, 113–130.e15.

Garcia-Beltran, W.F., St Denis, K.J., Hoelzemer, A., Lam, E.C., Nitido, A.D., Sheehan, M.L., Berrios, C., Ofoman, O., Chang, C.C., Hauser, B.M., et al. (2022). mRNA-based COVID-19 vaccine boosters induce neutralizing immunity against SARS-CoV-2 Omicron variant. Cell *185*, 457–466.e4.

Gilbert, P.B., Montefiori, D.C., McDermott, A.B., Fong, Y., Benkeser, D., Deng, W., Zhou, H., Houchens, C.R., Martins, K., Jayashankar, L., et al. (2021). Immune correlates analysis of the mRNA-1273 COVID-19 vaccine efficacy clinical trial. Science *375*, 43–50.

Goldberg, Y., Mandel, M., Bar-On, Y.M., Bodenheimer, O., Freedman, L., Haas, E.J., Milo, R., Alroy-Preis, S., Ash, N., and Huppert, A. (2021). Waning immunity after the BNT162b2 vaccine in Israel. N. Engl. J. Med. *385*, e85.

Gostic, K.M., Ambrose, M., Worobey, M., and Lloyd-Smith, J.O. (2016). Potent protection against H5N1 and H7N9 influenza via childhood hemagglutinin imprinting. Science *354*, 722–726.

Grabowski, F., Kochańczyk, M., and Lipniacki, T. (2022). The spread of SARS-CoV-2 variant omicron with a doubling time of 2.0–3.3 days can be explained by immune evasion. Viruses *14*, 294.

Halfmann, P.J., Iida, S., Iwatsuki-Horimoto, K., Maemura, T., Kiso, M., Scheaffer, S.M., Darling, T.L., Joshi, A., Loeber, S., Singh, G., et al. (2022). SARS-CoV-2 Omicron Virus Causes Attenuated Disease in Mice and Hamsters. Nature *603*, 687–692.

Hansen, C.H., Schelde, A.B., Moustsen-Helm, I.R., Emborg, H.-D., Krause, T.G., Mølbak, K., and Valentiner-Branth, P. (2021). Vaccine effectiveness against SARS-CoV-2 infection with the Omicron or Delta variants following a two-dose or booster BNT162b2 or mRNA-1273 vaccination series: A Danish cohort study. Preprint at medRxiv, 2021.2012.2020.21267966.

Hassett, K.J., Benenato, K.E., Jacquinet, E., Lee, A., Woods, A., Yuzhakov, O., Himansu, S., Deterling, J., Geilich, B.M., Ketova, T., et al. (2019). Optimization of lipid nanoparticles for intramuscular administration of mRNA vaccines. Mol. Ther. Nucleic Acids *15*, 1–11.

Hawman, D.W., Meade-White, K., Clancy, C., Archer, J., Hinkley, T., Leventhal, S.S., Rao, D., Stamper, A., Lewis, M., Rosenke, R., et al. (2022). Replicating RNA platform enables rapid response to the SARS-CoV-2 Omicron variant and elicits enhanced protection in naïve hamsters compared to ancestral vaccine. Preprint at bioRxiv, 2022.2001.2031.478520.

Hoffmann, M., Krüger, N., Schulz, S., Cossmann, A., Rocha, C., Kempf, A., Nehlmeier, I., Graichen, L., Moldenhauer, A.S., Winkler, M.S., et al. (2022). The Omicron variant is highly resistant against antibody-mediated neutralization: implications for control of the COVID-19 pandemic. Cell *185*, 447–456, e11.

Jackson, L.A., Anderson, E.J., Rouphael, N.G., Roberts, P.C., Makhene, M., Coler, R.N., McCullough, M.P., Chappell, J.D., Denison, M.R., Stevens, L.J., et al. (2020). An mRNA vaccine against SARS-CoV-2 - preliminary Report. N. Engl. J. Med. *383*, 1920–1931.

Johnston, R.J., Poholek, A.C., DiToro, D., Yusuf, I., Eto, D., Barnett, B., Dent, A.L., Craft, J., and Crotty, S. (2009). Bcl6 and Blimp-1 are reciprocal and antagonistic regulators of T follicular helper cell differentiation. Science *325*, 1006–1010.

Katzelnick, L.C., Coello Escoto, A., McElvany, B.D., Chávez, C., Salje, H., Luo, W., Rodriguez-Barraquer, I., Jarman, R., Durbin, A.P., Diehl, S.A., et al. (2018). Viridot: an automated virus plaque (immunofocus) counter for the measurement of serological neutralizing responses with application to dengue virus. PLoS Negl. Trop. Dis. *12*, e0006862.

Kim, D., Lee, J.Y., Yang, J.S., Kim, J.W., Kim, V.N., and Chang, H. (2020). The architecture of SARS-CoV-2 transcriptome. Cell *181*, 914–921.e10.

Köhler, H., Müller, S., and Nara, P.L. (1994). Deceptive imprinting in the immune response against HIV-1. Immunol. Today *15*, 475–478.

Lee, I.-J., Sun, C.-P., Wu, P.-Y., Lan, Y.-H., Wang, I.-H., Liu, W.-C., Tseng, S.-C., Tsung, S.-I., Chou, Y.-C., Kumari, M., et al. (2022). Omicron-specific mRNA vaccine induced potent neutralizing antibody against Omicron but not other SARS-CoV-2 variants. Preprint at bioRxiv, 2022.2001.2031.478406.

Maslo, C., Friedland, R., Toubkin, M., Laubscher, A., Akaloo, T., and Kama, B. (2022). Characteristics and outcomes of hospitalized patients in South Africa During the COVID-19 omicron wave compared With previous waves. JAMA *327*, 583–584.

Meng, B., Abdullahi, A., Ferreira, I.A.T.M., Goonawardane, N., Saito, A., Kimura, I., Yamasoba, D., Gerber, P.P., Fatihi, S., Rathore, S., et al. (2022). Altered TMPRSS2 usage by SARS-CoV-2 Omicron impacts infectivity and fusogenicity. Nature *603*, 706–714.

Muik, A., Lui, B.G., Wallisch, A.K., Bacher, M., Muhl, J., Reinholz, J., Ozhelvaci, O., Beckmann, N., Guimil Garcia, R.C., Poran, A., et al. (2022). Neutralization of SARS-CoV-2 Omicron by BNT162b2 mRNA vaccine-elicited human sera. Science *375*, eabn7591.

Naldini, L., Blömer, U., Gage, F.H., Trono, D., and Verma, I.M. (1996). Efficient transfer, integration, and sustained long-term expression of the transgene in adult rat brains injected with a lentiviral vector. Proc. Natl. Acad. Sci. USA *93*, 11382–11388.

Nurieva, R.I., Chung, Y., Martinez, G.J., Yang, X.O., Tanaka, S., Matskevitch, T.D., Wang, Y.H., and Dong, C. (2009). Bcl6 mediates the development of T follicular helper cells. Science *325*, 1001–1005.

Olia, A.S., Tsybovsky, Y., Chen, S.J., Liu, C., Nazzari, A.F., Ou, L., Wang, L., Kong, W.P., Leung, K., Liu, T., et al. (2021). SARS-CoV-2 S2P spike ages through distinct states with altered immunogenicity. J. Biol. Chem. *297*, 101127.

Pajon, R., Doria-Rose, N.A., Shen, X., Schmidt, S.D., O'Dell, S., McDanal, C., Feng, W., Tong, J., Eaton, A., Maglinao, M., et al. (2022). SARS-CoV-2 omicron variant neutralization after mRNA-1273 booster vaccination. N. Engl. J. Med. *386*, 1088–1091.

Pallesen, J., Wang, N., Corbett, K.S., Wrapp, D., Kirchdoerfer, R.N., Turner, H.L., Cottrell, C.A., Becker, M.M., Wang, L., Shi, W., et al. (2017). Immunogenicity and structures of a rationally designed prefusion MERS-CoV spike antigen. Proc. Natl. Acad. Sci. USA *114*, E7348–E7357.

Pilishvili, T., Gierke, R., Fleming-Dutra, K.E., Farrar, J.L., Mohr, N.M., Talan, D.A., Krishnadasan, A., Harland, K.K., Smithline, H.A., Hou, P.C., et al. (2021). Effectiveness of mRNA Covid-19 vaccine among U.S. Health care personnel. N. Engl. J. Med. *385*, e90.

Pinto, D., Park, Y.J., Beltramello, M., Walls, A.C., Tortorici, M.A., Bianchi, S., Jaconi, S., Culap, K., Zatta, F., De Marco, A., et al. (2020). Cross-neutralization of SARS-CoV-2 by a human monoclonal SARS-CoV antibody. Nature *583*, 290–295.

Planas, D., Veyer, D., Baidaliuk, A., Staropoli, I., Guivel-Benhassine, F., Rajah, M.M., Planchais, C., Porrot, F., Robillard, N., Puech, J., et al. (2021). Reduced sensitivity of SARS-CoV-2 variant Delta to antibody neutralization. Nature *596*, 276–280.

Polack, F.P., Thomas, S.J., Kitchin, N., Absalon, J., Gurtman, A., Lockhart, S., Perez, J.L., Pérez Marc, G., Moreira, E.D., Zerbini, C., et al. (2020). Safety and efficacy of the BNT162b2 mRNA Covid-19 vaccine. N. Engl. J. Med. *383*, 2603–2615.

Richardson, S.I., Madzorera, V.S., Spencer, H., Manamela, N.P., van der Mescht, M.A., Lambson, B.E., Oosthuysen, B., Ayres, F., Makhado, Z., Moyo-Gwete, T., et al. (2022). SARS-CoV-2 Omicron triggers cross-reactive neutralization and Fc effector functions in previously vaccinated, but not unvaccinated individuals. Preprint at medRxiv, 2022.2002.2010.22270789.

Rössler, A., Knabl, L., Laer, D.v., and Kimpel, J. (2022). Neutralization profile of Omicron variant convalescent individuals. Preprint at medRxiv, 2022.2002.2001.22270263.

Saunders, K.O., Lee, E., Parks, R., Martinez, D.R., Li, D., Chen, H., Edwards, R.J., Gobeil, S., Barr, M., Mansouri, K., et al. (2021). Neutralizing antibody vaccine for pandemic and pre-emergent coronaviruses. Nature *594*, 553–559.

Schmidt, F., Muecksch, F., Weisblum, Y., Da Silva, J., Bednarski, E., Cho, A., Wang, Z., Gaebler, C., Caskey, M., Nussenzweig, M.C., et al. (2022). Plasma neutralization of the SARS-CoV-2 omicron variant. N. Engl. J. Med. *386*, 599–601.

Shen, X., Tang, H., McDanal, C., Wagh, K., Fischer, W., Theiler, J., Yoon, H., Li, D., Haynes, B.F., Sanders, K.O., et al. (2021). SARS-CoV-2 variant B.1.1.7 is susceptible to neutralizing antibodies elicited by ancestral spike vaccines. Cell Host Microbe *29*, 529–539.e3.

Sigal, A. (2022). Milder disease with Omicron: is it the virus or the pre-existing immunity? Nat. Rev. Immunol. *22*, 69–71.

Sokal, A., Chappert, P., Barba-Spaeth, G., Roeser, A., Fourati, S., Azzaoui, I., Vandenberghe, A., Fernandez, I., Meola, A., Bouvier-Alias, M., et al. (2021). Maturation and persistence of the anti-SARS-CoV-2 memory B cell response. Cell *184*, 1201–1213.e14.

Suryawanshi, R.K., Chen, I.P., Ma, T., Syed, A.M., Simoneau, C.R., Ciling, A., Khalid, M.M., Sreekumar, B., Chen, P.-Y., George, A.F., et al. (2022). Limited cross-variant immunity after infection with the SARS-CoV-2 Omicron variant without vaccination. Preprint at medRxiv, 2022.2001.2013.22269243.

Tangye, S.G., Ferguson, A., Avery, D.T., Ma, C.S., and Hodgkin, P.D. (2002). Isotype switching by human B cells is division-associated and regulated by cytokines. J. Immunol. *169*, 4298–4306.

Teng, I.T., Nazzari, A.F., Choe, M., Liu, T., de Souza, M.O., Petrova, Y., Tsybovsky, Y., Wang, S., Zhang, B., Artamonov, M., et al. (2021). Molecular probes of spike ectodomain and its subdomains for SARS-CoV-2 variants, Alpha through Omicron. Preprint at bioRxiv, 2021.2012.2029.474491.

Tseng, H.F., Ackerson, B.K., Luo, Y., Sy, L.S., Talarico, C.A., Tian, Y., Bruxvoort, K.J., Tubert, J.E., Florea, A., Ku, J.H., et al. (2022). Effectiveness of mRNA-1273 against SARS-CoV-2 Omicron and Delta variants. Nat. Med.

Published online February *21*, 2022. https://doi.org/10.1038/s41591-022-01753-y.

VanBlargan, L.A., Errico, J.M., Halfmann, P.J., Zost, S.J., Crowe, J.E., Jr., Purcell, L.A., Kawaoka, Y., Corti, D., Fremont, D.H., and Diamond, M.S. (2022). An infectious SARS-CoV-2 B.1.1.529 Omicron virus escapes neutralization by therapeutic monoclonal antibodies. Nat. Med. *28*, 490–495.

Vanderheiden, A., Edara, V.V., Floyd, K., Kauffman, R.C., Mantus, G., Anderson, E., Rouphael, N., Edupuganti, S., Shi, P.Y., Menachery, V.D., et al. (2020). Development of a rapid focus reduction neutralization test assay for measuring SARS-CoV-2 neutralizing antibodies. Curr. Protoc. Immunol. *131*, e116.

Vanderheiden, A., Thomas, J., Soung, A.L., Davis-Gardner, M.E., Floyd, K., Jin, F., Cowan, D.A., Pellegrini, K., Shi, P.Y., Grakoui, A., et al. (2021). CCR2 signaling restricts SARS-CoV-2 infection. mBio *12*, e0274921.

Viana, R., Moyo, S., Amoako, D.G., Tegally, H., Scheepers, C., Althaus, C.L., Anyaneji, U.J., Bester, P.A., Boni, M.F., Chand, M., et al. (2022). Rapid Epidemic Expansion of the SARS-CoV-2 Omicron Variant in Southern Africa. Nature *603*, 679–686.

Wang, R., Zhang, Q., Ge, J., Ren, W., Zhang, R., Lan, J., Ju, B., Su, B., Yu, F., Chen, P., et al. (2021). Analysis of SARS-CoV-2 variant mutations reveals neutralization escape mechanisms and the ability to use ACE2 receptors from additional species. Immunity *54*, 1611–1621.e5.

Wang, L., Zhou, T., Zhang, Y., Yang, E.S., Schramm, C.A., Shi, W., Pegu, A., Oloniniyi, O.K., Henry, A.R., Darko, S., et al. (2021). Ultrapotent antibodies against diverse and highly transmissible SARS-CoV-2 variants. Science *373*, eabh1766.

Willett, B.J., Grove, J., MacLean, O.A., Wilkie, C., Logan, N., Lorenzo, G.D., Furnon, W., Scott, S., Manali, M., Szemiel, A., et al. (2022). The hyper-transmissible SARS-CoV-2 Omicron variant exhibits significant antigenic change, vaccine escape and a switch in cell entry mechanism. Preprint at medRxiv, 2022.2001.2003.21268111.

Wölfel, R., Corman, V.M., Guggemos, W., Seilmaier, M., Zange, S., Müller, M.A., Niemeyer, D., Jones, T.C., Vollmar, P., Rothe, C., et al. (2020). Virological assessment of hospitalized patients with COVID-2019. Nature *581*, 465–469.

Wolter, N., Jassat, W., Walaza, S., Welch, R., Moultrie, H., Groome, M., Amoako, D.G., Everatt, J., Bhiman, J.N., Scheepers, C., et al. (2022). Early assessment of the clinical severity of the SARS-CoV-2 omicron variant in South Africa: a data linkage study. Lancet *399*, 437–446.

Worobey, M., Han, G.Z., and Rambaut, A. (2014). Genesis and pathogenesis of the 1918 pandemic H1N1 influenza A virus. Proc. Natl. Acad. Sci. USA *111*, 8107–8112.

Wrapp, D., Wang, N., Corbett, K.S., Goldsmith, J.A., Hsieh, C.L., Abiona, O., Graham, B.S., and McLellan, J.S. (2020). Cryo-EM structure of the 2019-nCoV spike in the prefusion conformation. Science *367*, 1260–1263.

Zhou, T., Teng, I.T., Olia, A.S., Cerutti, G., Gorman, J., Nazzari, A., Shi, W., Tsybovsky, Y., Wang, L., Wang, S., et al. (2020). Structure-based design with tag-based purification and in-process biotinylation enable streamlined development of SARS-CoV-2 spike Molecular Probes. Cell Rep. *33*, 108322.

STAR★METHODS

KEY RESOURCES TABLE

REAGENT or RESOURCE	SOURCE	IDENTIFIER
Antibodies		
SARS-CoV-2 spike antibody (biotin, CR3022)	Novus Biologicals	Cat#CR3022; RRID:AB_2848080
Goat anti-monkey IgG (H+L) secondary antibody, HRP (polyclonal)	Invitrogen	Cat#PA1-84631; RRID:AB_933605
B1-182	Vaccine Research Center, NIH (Wang et al., 2021a)	N/A
A19-46.1	Vaccine Research Center, NIH (Wang et al., 2021a)	N/A
A19-61.1	Vaccine Research Center, NIH (Wang et al., 2021a)	N/A
S309	(Pinto et al., 2020)	N/A
A23-97.1	Vaccine Research Center, NIH (Corbett et al., 2021a)	N/A
A23-80.1	Vaccine Research Center, NIH (Corbett et al., 2021a)	N/A
Goat anti-human IgD-FITC (polyclonal)	Southern Biotech	Cat#2030-02; RRID:AB_2795624
PerCP-Cy5.5 mouse anti-human IgM (clone G20-127)	BD Biosciences	Cat#561285; RRID:AB_10611998
DyLight 405 AffiniPure goat anti-human serum IgA, α chain specific (polyclonal)	Jackson ImmunoResearch	Cat#109-475-011; RRID:AB_2337789
Brilliant Violet 570 anti-human CD20 antibody (clone 2H7)	Biolegend	Cat#302332; RRID:AB_2563805
Brilliant Violet 650 anti-human CD27 antibody (clone O323)	Biolegend	Cat#302828; RRID:AB_2562096
Brilliant Violet 785 anti-human CD14 antibody (clone M5E2)	Biolegend	Cat#301840; RRID:AB_2563425
BUV496 mouse anti-human CD16 (clone 3G8)	BD Biosciences	Cat#612944; RRID:AB_2870224
BUV737 mouse anti-human CD4 (clone SK3)	BD Biosciences	Cat#612748; RRID:AB_2870079
CD19-APC (clone J3-119)	Beckman Coulter	Cat#IM2470U
Alexa Fluor 700 mouse anti-human IgG (clone G18-145)	BD Biosciences	Cat#561296; RRID:AB_10612406
APC-Cy7 mouse anti-human CD3 (clone SP34-2)	BD Biosciences	Cat#557757; RRID:AB_396863
Anti-human CD38 PE (clone OKT10)	Caprico Biotechnologies	Cat#100826
PE-Cy5 mouse anti-human CD21 (clone B-ly4)	BD Biosciences	Cat#551064; RRID:AB_394028
Mouse anti-human CD185 (CXCR5) monoclonal antibody, PE-Cyanine7, eBioscience (clone MU5UBEE)	ThermoFisher Scientific	Cat#25-9185-42; RRID:AB_2573540
Mouse anti-human CD4 monoclonal antibody, PE-Cyanine5.5 (clone S3.5)	ThermoFisher Scientific	Cat#MHCD0418; RRID:AB_10376013
Brilliant Violet 570 anti-human CD8a antibody (clone RPA-T8)	Biolegend	Cat#301038; RRID:AB_2563213
PE-Cy5 mouse anti-human CD45RA (clone 5H9)	BD Biosciences	Cat#552888; RRID:AB_394517
Brilliant Violet 650 anti-human CD197 (CCR7) antibody (clone G043H7)	Biolegend	Cat#353234; RRID:AB_2563867
Mouse anti-human CD185 (CXCR5) monoclonal antibody, PE, eBioscience (clone MU5UBEE)	ThermoFisher Scientific	Cat#12-9185-42; RRID:AB_11219877
BV711 mouse anti-human CD183 (clone 1C6/CXCR3)	BD Biosciences	Cat#563156; RRID:AB_2738034

(*Continued on next page*)

Continued

REAGENT or RESOURCE	SOURCE	IDENTIFIER
BUV737 mouse anti-human CD279 (PD-1) (clone EH12.1)	BD Biosciences	Cat#565299; RRID:AB_2739167
PE/Cyanine7 anti-human/mouse/rat CD278 (ICOS) antibody (clone C398.4A)	Biolegend	Cat#313520; RRID:AB_10643411
Mouse anti-human CD69-ECD, RUO (clone TP1.55.3)	Beckman Coulter	Cat#6607110; RRID:AB_1575978
Alexa Fluor 700 anti-human IFN-γ antibody (clone B27)	Biolegend	Cat#506516; RRID:AB_961351
BV750 rat anti-human IL-2 (clone MQ1-17H12)	BD Biosciences	Cat#566361; RRID:AB_2739710
High parameter custom BB700 conjugate (rat anti-human IL-4) (clone MP4-25D2)	BD Biosciences	Cat#624381
FITC mouse anti-human TNF (clone MAb11)	BD Biosciences	Cat#554512; RRID:AB_395443
BV421 rat anti-human IL-13 (clone JES10-5A2)	BD Biosciences	Cat#563580; RRID:AB_2738290
Brilliant Violet 605 anti-human IL-17A antibody (clone BL168)	Biolegend	Cat#512326; RRID:AB_2563887
Alexa Fluor 647 mouse anti-human IL-21 (clone 3A3-N2.1)	BD Biosciences	Cat#560493; RRID:AB_1645421
Brilliant Violet 785 anti-human CD154 antibody (clone 24-31)	Biolegend	Cat#310842; RRID:AB_2572187
SARS-CoV-2 (COVID-19) nucleocapsid antibody (polyclonal)	GeneTex	Cat#GTX135357; RRID:AB_2868464
Bacterial and virus strains		
SARS-CoV-2 B.1.1.529 (challenge stock)	This paper	N/A
SARS-CoV-2 D614G (EHC-083E)	Mehul Suthar, Emory (Edara et al., 2021a)	N/A
SARS-CoV-2 B.1.351	Mehul Suthar, Emory (Vanderheiden et al., 2021)	N/A
SARS-CoV-2 B.1.617.2	Mehul Suthar, Emory (Edara et al., 2021b)	N/A
SARS-CoV-2 B.1.1.529 (neutralization assay)	Mehul Suthar, Emory (Edara et al., 2022)	N/A
Chemicals, peptides, and recombinant proteins		
SARS-CoV2-WT-S2P-AVI-bio	Vaccine Research Center, NIH (Zhou et al., 2020)	N/A
SARS-CoV2-D614G-S2P-AVI-bio	Vaccine Research Center, NIH (Teng et al., 2021)	N/A
SARS-CoV2-B.1.351-S2P-AVI-bio	Vaccine Research Center, NIH (Teng et al., 2021)	N/A
SARS-CoV2-B.1.617.2-S2P-AVI-bio	Vaccine Research Center, NIH (Teng et al., 2021)	N/A
SARS-CoV2-B.1.1.529-S2P-AVI-bio	Vaccine Research Center, NIH (Teng et al., 2021)	N/A
MSD blocker A kit	Meso Scale Diagnostics	Cat#R93AA
MSD SULFO-TAG human ACE2 protein (included in kit)	Meso Scale Diagnostics	Cat#K15586U
MSD GOLD read buffer B	Meso Scale Diagnostics	Cat#R60AM
MSD diluent 100	Meso Scale Diagnostics	Cat#R50AA
Lipofectamine 3000 transfection reagent	ThermoFisher Scientific	Cat#L3000075
FuGENE 6 transfection reagent	Promega	Cat#E2691
Luciferase assay system	Promega	Cat#E1500
SARS-CoV-2 S-2P (Avidity and Epitope Mapping)	Vaccine Research Center, NIH (Corbett et al., 2021b; Francica et al., 2021)	N/A
SARS-CoV-2 B.1.1.529 S-2P (Avidity and Epitope Mapping)	Vaccine Research Center, NIH	N/A
Sodium thiocyanate solution	Millipore-Sigma	Cat#80518-500ML-F

(*Continued on next page*)

Continued

REAGENT or RESOURCE	SOURCE	IDENTIFIER
BV605 Streptavidin	BD Biosciences	Cat#563260
BUV661 Streptavidin	BD Biosciences	Cat#612979
LIVE/DEAD Fixable Aqua Dead Cell Stain Kit	ThermoFisher Scientific	Cat#L34966
PepMix SARS-CoV-2 (S1+S2) (custom p.K986P and p.V987P)	JPT Peptide Techologies	N/A
PepMix SARS-CoV-2 (Spike B.1.1.529 / Omicron)	JPT Peptide Techologies	Cat#PM-SARS2-SMUT08-1
Critical commercial assays		
NEBNext ultra II RNA library prep kit for Illumina	New England Biolabs	Cat#E7770
NEBNext multiplex oligos	New England Biolabs	Cat#E6440
V-PLEX SARS-CoV-2 panel 22 (IgG) kit	Meso Scale Diagnostics	Cat#K15559U
V-PLEX SARS-CoV-2 panel 23 (IgG) kit	Meso Scale Diagnostics	Cat#K15567U
Britelite plus reporter gene assay system	PerkinElmer	Cat#6066769
His capture kit type 2	Cytiva	Cat#29234602
Amine coupling kit	Cytiva	Cat#BR100633
Series S sensor chip CM5	Cytiva	Cat#29149603
RNAzol BD Column Kit	Molecular Research Center	Cat#RC 292
TaqMan Fast Virus 1-Step Master Mix	ThermoFisher Scientific	Cat#4444436
Experimental models: Cell lines		
Vero (clone E6)	ATCC	Cat#CRL-1586; RRID:CVCL_0574
VeroE6-TMPRSS2	Vaccine Research Center, NIH (Corbett et al., 2021c)	N/A
HEK-293T/17	ATCC	Cat#CRL-11268; RRID:CVCL_1926
HEK-293T-ACE2	Michael Farzan and Huihui Mu, Scripps Research	N/A
Experimental models: Organisms/strains		
Indian-origin rhesus macaques	Vaccine Research Center, NIH	N/A
Oligonucleotides		
Primer: sgLeadSARSCoV2_F: 5'-CGATCTCT TGTAGATCTGTTCTC-3'	Integrated DNA Technologies (Francica et al., 2021; Wolfel et al., 2020)	N/A
Probe: N2_P: 5'-FAM- CGATCAAAACAA CGTCGGCCCC-BHQ1 -3'	This paper	N/A
Primer: wtN_R: 5'-GGTGAACCAAGACGCA GTAT-3'	Integrated DNA Technologies (Corbett et al., 2021c; Saunders et al., 2021)	N/A
Recombinant DNA		
VRC5601: pHR'CMV Luc	(Naldini et al., 1996)	N/A
VRC5602: pCMV ΔR8.2	(Naldini et al., 1996)	N/A
VRC9260: TMPRSS2	Vaccine Research Center, NIH (DiPiazza et al., 2021)	N/A
Spike_SARS-CoV-2 D614G	Vaccine Research Center, NIH (Corbett et al., 2021a)	N/A
Spike_SARS-CoV-2 B.1.351	Vaccine Research Center, NIH (Corbett et al., 2021a)	N/A
Spike_SARS-CoV-2 B.1.617.2	Vaccine Research Center, NIH (Corbett et al., 2021a)	N/A
Spike_SARS-CoV-2 B.1.1.529	Vaccine Research Center, NIH	N/A
Software and algorithms		
CLC Genomics Workbench v.21.0.3	Qiagen	https://digitalinsights.qiagen.com/downloads/product-downloads/
Viridot program	(Katzelnick et al., 2018)	https://github.com/leahkatzelnick/Viridot

(*Continued on next page*)

Continued

REAGENT or RESOURCE	SOURCE	IDENTIFIER
GraphPad Prism v8.2.0, v9.0.2, v9.2.0	GraphPad	https://www.graphpad.com/scientific-software/prism/
Biacore Insight Evaluation Software	Cytiva	Cat#29310602
FlowJo v10.7.2, v10.8.0	Becton Dickinson	https://www.flowjo.com
R v4.1.0	The R Foundation	https://www.r-project.org
Other		
Amicon Ultra-15 centrifugal filter unit (50,000 MWCO)	Millipore Sigma	Cat#UFC905096
Streptavidin multi array 384 well plate	Meso Scale Diagnostics	Cat#L21SA-1

RESOURCE AVAILABILITY

Lead contact

Further information and requests for resources should be directed to and will be fulfilled by the lead contact, Robert A. Seder (rseder@mail.nih.gov).

Materials availability

This study did not generate new unique reagents.

Data and code availability

All data reported in this paper will be shared by the lead contact upon request.

This paper does not report original code.

Any additional information required to reanalyze the data reported in this paper is available from the lead contact upon request.

EXPERIMENTAL MODEL AND SUBJECT DETAILS

Preclinical mRNA and lipid nanoparticles

A sequence-optimized mRNA encoding prefusion-stabilized SARS-CoV-2 S protein containing 2 proline stabilization mutations (S-2P) (Pallesen et al., 2017; Wrapp et al., 2020) for WA1, Omicron, and Beta were synthesized in vitro and formulated (Hassett et al., 2019). Control mRNA "UNFIX-01 (Untranslated Factor 9)" was synthesized and similarly formulated into lipid nanoparticles as previously described (Corbett et al., 2021a).

Rhesus macaque model and immunizations

All experiments conducted according to NIH regulations and standards on the humane care and use of laboratory animals as well as the Animal Care and Use Committees of the NIH Vaccine Research Center and BIOQUAL, Inc. (Rockville, Maryland). All studies were conducted at BIOQUAL, Inc. Four- to eight-year-old rhesus macaques of Indian origin were stratified into groups based on sex, age, and weight. Eight macaques were immunized with mRNA-1273 at weeks 0 and 4 with a dose of 100μg delivered intramuscularly in 1mL of formulated lipid nanoparticles diluted in phosphate-buffered saline (PBS) into the right quadricep as previously described (Corbett et al., 2020, 2021c; Gagne et al., 2022). At week 41 (~9 months after the second immunization), the eight macaques were split into two groups of 4 and boosted with 50μg mRNA-1273 or 50μg mRNA-Omicron. Animals in the control group were immunized with 50μg control mRNA at the time of the boost.

For comparisons of variant-matched vaccines as a primary immunization regimen, two additional groups of 8 macaques (three- to eight-years old) were immunized with either 100μg mRNA-Omicron or 50μg mRNA-Beta at weeks 0 and 4 according to the process described above. Two weeks following the second dose, sera were collected for analysis of neutralizing antibody responses.

METHOD DETAILS

Cells and viruses

VeroE6-TMPRSS2 cells were generated at the Vaccine Research Center, NIH, Bethesda, MD. Isolation and sequencing of EHC-083E (D614G SARS-CoV-2), Delta, Beta, and Omicron for live virus neutralization assays were previously described (Edara et al., 2022, 2021a, 2021b; Vanderheiden et al., 2020). Viruses were propagated in Vero-TMPRSS2 cells to generate viral stocks. Viral titers were determined by focus-forming assay on VeroE6-TMPRSS2 cells. Viral stocks were stored at -80°C until use.

Sequencing of Omicron virus stock

NEBNext Ultra II RNA Prep reagents and multiplex oligos (New England Biolabs) were used to prepare Illumina-ready libraries, which were sequenced on a MiSeq (Illumina) as described previously (Corbett et al., 2021c; Gagne et al., 2022). Demultiplexed sequence reads were analyzed in the CLC Genomics Workbench v.21.0.3 by (1) trimming for quality, length, and adaptor sequence, (2) mapping to the Wuhan-Hu-1 SARS-CoV-2 reference (GenBank no. NC_045512), (3) improving the mapping by local realignment in areas containing insertions and deletions (indels), and (4) generating both a sample consensus sequence and a list of variants. Default settings were used for all tools.

Omicron challenge

Macaques were challenged at week 45 (4 weeks after the second boost) with a total dose of 1×10^6 PFU of SARS-CoV-2 Omicron. The viral inoculum was administered as 7.5×10^5 PFU in 3mL intratracheally and 2.5×10^5 PFU in 1mL intranasally in a volume of 0.5mL distributed evenly into each nostril.

Serum and mucosal antibody titers

Quantification of antibodies in the blood and mucosa were performed as previously described (Corbett et al., 2020). Briefly, total IgG antigen-specific antibodies to variant SARS-CoV-2 S- and RBD-derived antigens were determined in a multiplex serology assay by Meso Scale Discovery (MSD) V-Plex SARS-CoV-2 Panel 23 for S and MSD V-Plex SARS-CoV-2 Panel 22 for RBD according to manufacturer's instructions, except 25μl of sample and detection antibody were used per well. Heat inactivated plasma was initially diluted 1:100 and then serially diluted 1:10 for blood S- and 1:4 for RBD-binding. BAL fluid and nasal washes were concentrated 10-fold with Amicon Ultra centrifugal filter devices (Millipore Sigma). Concentrated samples were diluted 1:5 prior to 5-fold serial dilutions.

S-2P antigens

While S antigens were used for binding ELISAs, S-2P antigens were used for ACE2 inhibition assays and B cell probe binding. S-2P constructs were made as follows. Biotinylated S probes were expressed transiently for WA1, D614G, Delta, Beta, and Omicron strains and purified and biotinylated in a single in-process step (Teng et al., 2021; Zhou et al., 2020). S-2P for WA1 and Omicron were made as previously described (Olia et al., 2021).

S-2P-ACE2 binding inhibition

ACE2 binding inhibition was performed using a modified MSD platform assay. Briefly, after blocking MSD Streptavidin MULTI-ARRAY 384 well plates with Blocker A (MSD), the plates were coated with 1 μg/ml of biotinylated SARS-CoV-2 variant S-2P (D614G, Beta, Delta, or Omicron) and incubated for 1 hour at room temperature (RT). The plates were washed 5 times with wash buffer (1x PBS containing 0.05% Tween-20). Diluted samples were added to the coated plates and incubated for 1 hour at RT. MSD SULFO-TAG human ACE2 protein was diluted 1:200 and added to the plates. After 1 hour incubation at RT, the plates were washed 5 times with wash buffer and read on MSD Sector S 600 instrument after the addition of Gold Read Buffer B (MSD). Results are reported as percent inhibition. BAL fluid and nasal washes were first concentrated 10-fold with Amicon Ultra centrifugal filter devices (Millipore Sigma) and then diluted 1:5 in Diluent 100 (MSD).

Focus reduction neutralization assay

FRNT assays were performed as previously described (Edara et al., 2021a, 2021b; Vanderheiden et al., 2020). Briefly, samples were diluted at 3-fold in 8 serial dilutions using DMEM (VWR, #45000-304) in duplicates with an initial dilution of 1:10 in a total volume of 60μl. Serially diluted samples were incubated with an equal volume of D614G, Delta, Beta, or Omicron (100-200 foci per well based on the target cell) at 37°C for 45 minutes in a round-bottomed 96-well culture plate. The antibody-virus mixture was then added to VeroE6-TMPRSS2 cells and incubated at 37°C for 1 hour. Post-incubation, the antibody-virus mixture was removed and 100μl of pre-warmed 0.85% methylcellulose overlay was added to each well. Plates were incubated at 37°C for 18 hours and the methylcellulose overlay was removed and washed six times with PBS. Cells were fixed with 2% paraformaldehyde in PBS for 30 minutes. Following fixation, plates were washed twice with PBS and permeabilization buffer (0.1% BSA, 0.1% Saponin in PBS) was added to cells for at least 20 minutes. Cells were incubated with an anti-SARS-CoV S primary antibody directly conjugated to Alexaflour-647 (CR3022-AF647) overnight at 4°C. Foci were visualized and imaged on an ELISPOT reader (CTL). Antibody neutralization was quantified by counting the number of foci for each sample using the Viridot program (Katzelnick et al., 2018). The neutralization titers were calculated as follows: 1 - (ratio of the mean number of foci in the presence of sera and foci at the highest dilution of respective sera sample). Each specimen was tested in duplicate. The FRNT-50 titers were interpolated using a 4-parameter nonlinear regression in GraphPad Prism v9.2.0. Samples that do not neutralize at the limit of detection (LOD) at 50% were plotted at 20, which was used for geometric mean and fold-change calculations. The assay LOD was 20.

Lentiviral pseudovirus neutralization

For comparison of boost cohorts, neutralizing antibodies in serum or plasma were measured in a validated pseudovirus-based assay as a function of reductions in luciferase reporter gene expression after a single round of infection with SARS-CoV-2 spike-pseudotyped viruses in 293T/ACE2 cells (293T cell line stably overexpressing the human ACE2 cell surface receptor protein, obtained from

Drs. Michael Farzan and Huihui Mu at Scripps) as previously described (Gilbert et al., 2021; Shen et al., 2021). SARS-CoV-2 S-pseudotyped virus was prepared by transfection using Lipofectamine 3000 (ThermoFisher, #L3000075) in 293T/17 cells (human embryonic kidney cells in origin; obtained from American Type Culture Collection, #CRL-11268) using a lentivirus backbone vector, a spike-expression plasmid encoding S protein from Wuhan-Hu-1 strain (GenBank no. NC_045512) with a p.Asp614Gly mutation, a TMPRSS2 expression plasmid, and a firefly Luc reporter plasmid. For pseudovirus encoding the S from Delta, Beta, and Omicron, the plasmid was altered via site-directed mutagenesis to match the S sequence to the corresponding variant sequence as previously described (Corbett et al., 2021a). A pre-titrated dose of pseudovirus was incubated with eight serial 5-fold dilutions of serum samples (1:20 start dilution) in duplicate in 384-well flat-bottom tissue culture plates (Thermo Fisher, #12-565-344) for 1 hour at 37°C prior to adding 293T/ACE2 cells. One set of 14 wells received cells and virus (virus control) and another set of 14 wells received cells only (background control), corresponding to technical replicates. Luminescence was measured after 66-72 hours of incubation using Britelite-Plus luciferase reagent (PerkinElmer, #6066769). Neutralization titers are the inhibitory dilution of serum samples at which relative luminescence units (RLUs) were reduced by 50% (ID_{50}) compared to virus control wells after subtraction of background RLUs. Serum samples were heat-inactivated for 45-60 minutes at 56°C prior to assay.

For pseudovirus assay using samples from variant-matched primary immunization regimens, a similar protocol was used with the following modifications. Pseudoviruses were prepared by transfection with FuGENE 6 transfection reagent (Promega, #E2691). A pre-titrated dose of pseudovirus was incubated with 4-fold dilutions of serum samples (1:40 start dilution) in duplicate in 96-well tissue culture isoplates (PerkinElmer, #6005060) for 1 hour at 37°C prior to adding 293T/ACE2 cells. Luminescence was measured after 72 hours of incubation using Luciferase Assay System (Promega, #E1500). ID_{50} titers were calculated using a log(agonist) versus normalized-response (variable slope) nonlinear regression model in Prism v9.0.2 (GraphPad). For samples that did not neutralize at the limit of detection at 50%, a value of 20 was plotted and used for geometric mean calculations.

Serum antibody avidity

Avidity was measured as described previously (Francica et al., 2021) in an adapted ELISA assay. Briefly, ELISA against S-2P was performed in the absence or presence of sodium thiocyanate (NaSCN) and developed with HRP-conjugated goat anti-monkey IgG (H+L) secondary antibody (Invitrogen) and SureBlue 3,3′,5,5′-tetramethylbenzidine (TMB) microwell peroxidase substrate (1-Component; SeraCare) and quenched with 1N H_2SO_4. The avidity index (AI) was calculated as the ratio of IgG binding to S-2P in the absence or presence of NaSCN.

Epitope mapping

Serum epitope mapping competition assays were performed, as previously described (Corbett et al., 2021a), using the Biacore 8K+ surface plasmon resonance system (Cytiva). Briefly, through primary amine coupling using a His capture kit (Cytiva), anti-histidine antibody was immobilized on Series S Sensor Chip CM5 (Cytiva) allowing for the capture of his-tagged SARS-CoV-2 S-2P on active sensor surface.

Human IgG monoclonal antibodies (mAbs) used for these analyses include: RBD-specific mAbs B1-182, A19-46.1, A19-61.1, S309, A23-97.1, and A23-80.1. Negative control antibody or competitor mAb was injected over both active and reference surfaces. Following this, NHP sera (diluted 1:50) was flowed over both active and reference sensor surfaces. Active and reference sensor surfaces were regenerated between each analysis cycle.

For analysis, sensorgrams were aligned to Y (Response Units) = 0, using Biacore 8K Insights Evaluation Software (Cytiva) beginning at the serum association phase. Relative ''analyte binding late'' report points (RU) were collected and used to calculate fractional competition (% C) using the following formula: % C = [1 – (100 * ((RU in presence of competitor mAb) / (RU in presence of negative control mAb)))]. Results are reported as fractional competition. Assays were performed in duplicate, with average data point represented on corresponding graphs.

B cell probe binding

Kinetics of S-specific memory B cells responses were determined as previously described (Gagne et al., 2022). Briefly, cryopreserved PBMC were thawed and stained with the following antibodies (monoclonal unless indicated): IgD FITC (goat polyclonal, Southern Biotech), IgM PerCP-Cy5.5 (clone G20-127, BD Biosciences), IgA Dylight 405 (goat polyclonal, Jackson Immunoresearch Inc), CD20 BV570 (clone 2H7, Biolegend), CD27 BV650 (clone O323, Biolegend), CD14 BV785 (clone M5E2, Biolegend), CD16 BUV496 (clone 3G8, BD Biosciences), CD4 BUV737 (clone SK3, BD Biosciences), CD19 APC (clone J3-119, Beckman), IgG Alexa 700 (clone G18-145, BD Biosciences), CD3 APC-Cy7 (clone SP34-2, BD Biosciences), CD38 PE (clone OKT10, Caprico Biotechnologies), CD21 PE-Cy5 (clone B-ly4, BD Biosciences), and CXCR5 PE-Cy7 (clone MU5UBEE, Thermo Fisher Scientific). Stained cells were then incubated with streptavidin-BV605 (BD Biosciences) labeled WA1, Beta, Delta, or Omicron S-2P and streptavidin-BUV661 (BD Biosciences) labeled WA1 or Delta S-2P for 30 minutes at 4°C (protected from light). Cells were washed and fixed in 0.5% formaldehyde (Tousimis Research Corp) prior to data acquisition. Aqua live/dead fixable dead cell stain kit (Thermo Fisher Scientific) was used to exclude dead cells. All antibodies were previously titrated to determine the optimal concentration. Samples were acquired on an BD FACSymphony cytometer and analyzed using FlowJo version 10.7.2 (BD, Ashland, OR).

Intracellular cytokine staining

Intracellular cytokine staining was performed as previously described (Donaldson et al., 2019; Gagne et al., 2022). Briefly, cryopreserved PBMC and BAL cells were thawed and rested overnight in a 37°C/5% CO_2 incubator. The following morning, cells were stimulated with SARS-CoV-2 S protein peptide pools (S1 and S2, matched to vaccine insert or Omicron variant; JPT Peptides) at a final concentration of 2 μg/ml in the presence of 3mM monensin for 6 hours. Both sets of S1 and S2 peptide pools were comprised of 158 and 157 individual peptides, respectively, as 15 mers overlapping by 11 amino acids in 100% DMSO. Negative controls received an equal concentration of DMSO instead of peptides (final concentration of 0.5%). The following monoclonal antibodies were used: CD3 APC-Cy7 (clone SP34-2, BD Biosciences), CD4 PE-Cy5.5 (clone S3.5, Invitrogen), CD8 BV570 (clone RPA-T8, BioLegend), CD45RA PE-Cy5 (clone 5H9, BD Biosciences), CCR7 BV650 (clone G043H7, BioLegend), CXCR5 PE (clone MU5UBEE, Thermo Fisher), CXCR3 BV711 (clone 1C6/CXCR3, BD Biosciences), PD-1 BUV737 (clone EH12.1, BD Biosciences), ICOS Pe-Cy7 (clone C398.4A, BioLegend), CD69 ECD (cloneTP1.55.3, Beckman Coulter), IFN-g Ax700 (clone B27, BioLegend), IL-2 BV750 (clone MQ1-17H12, BD Biosciences), IL-4 BB700 (clone MP4-25D2, BD Biosciences), TNF-FITC (clone Mab11, BD Biosciences), IL-13 BV421 (clone JES10-5A2, BD Biosciences), IL-17 BV605 (clone BL168, BioLegend), IL-21 Ax647 (clone 3A3-N2.1, BD Biosciences), and CD154 BV785 (clone 24-31, BioLegend). Aqua live/dead fixable dead cell stain kit (Thermo Fisher Scientific) was used to exclude dead cells. All antibodies were previously titrated to determine the optimal concentration. Samples were acquired on a BD FACSymphony flow cytometer and analyzed using FlowJo version 10.8.0 (BD, Ashland, OR).

Subgenomic RNA quantification

sgRNA was isolated and quantified by researchers blinded to vaccine status as previously described (Corbett et al., 2021c), except for the use of a new probe noted below. Briefly, total RNA was extracted from BAL fluid and nasal swabs using RNAzol BD column kit (Molecular Research Center). PCR reactions were conducted with TaqMan Fast Virus 1-Step Master Mix (Applied Biosystems), forward primer in the 5' leader region and gene-specific probes and reverse primers as follows:

sgLeadSARSCoV2_F: 5'-CGATCTCTTGTAGATCTGTTCTC-3'

N gene

N2_P: 5'-FAM- CGATCAAAACAACGTCGGCCCC-BHQ1-3'

wtN_R: 5'-GGTGAACCAAGACGCAGTAT-3'

Amplifications were performed with a QuantStudio 6 Pro Real-Time PCR System (Applied Biosystems). The assay lower LOD was 50 copies per reaction.

$TCID_{50}$ assay

$TCID_{50}$ was quantified as previously described (Corbett et al., 2021c). Briefly, Vero-TMPRSS2 cells were plated and incubated overnight. The following day, BAL or NS samples were serially diluted, and the plates were incubated at 37 °C/5.0% CO_2 for four days. Positive (virus stock of known infectious titer in the assay) and negative (medium only) control wells were included in each assay setup. The cell monolayers were visually inspected for cytopathic effect. $TCID_{50}$ values were calculated using the Reed–Muench formula.

Histopathology and immunohistochemistry

Routine histopathology and detection of SARS-CoV-2 virus antigen via immunohistochemistry (IHC) were performed as previously described (Corbett et al., 2020; Gagne et al., 2022). Briefly, 8 days following Omicron challenge, animals were euthanized and lung tissue was processed and stained with hematoxylin and eosin for pathological analysis or with a rabbit polyclonal anti-SARS-CoV-2 anti-nucleocapsid antibody (GeneTex, GTX135357) at a dilution of 1:2000 for IHC. Tissue sections were analyzed by a blinded board-certified veterinary pathologist using an Olympus BX43 light microscope. Photomicrographs were taken on an Olympus DP27 camera.

QUANTIFICATION AND STATISTICAL ANALYSIS

Comparisons between groups, or between timepoints within a group, are based on unpaired and paired t-tests, respectively. Binding, neutralizing, and viral assays are log-transformed as appropriate and reported with geometric means and corresponding geometric standard deviations where indicated. There are no adjustments for multiple comparisons, so all p values should be interpreted as suggestive rather than conclusive. All analyses are conducted using R version 4.1.0 and GraphPad Prism version 8.2.0 unless otherwise specified.

p values are shown in the figures, and the sample *n* is listed in corresponding figure legends. For all data presented, n=4 for individual boost cohorts and n=4-8 for controls and vaccinated NHP at pre-boost timepoints. NS denotes that the indicated comparison was not significant, with P>0.05.

Supplemental figures

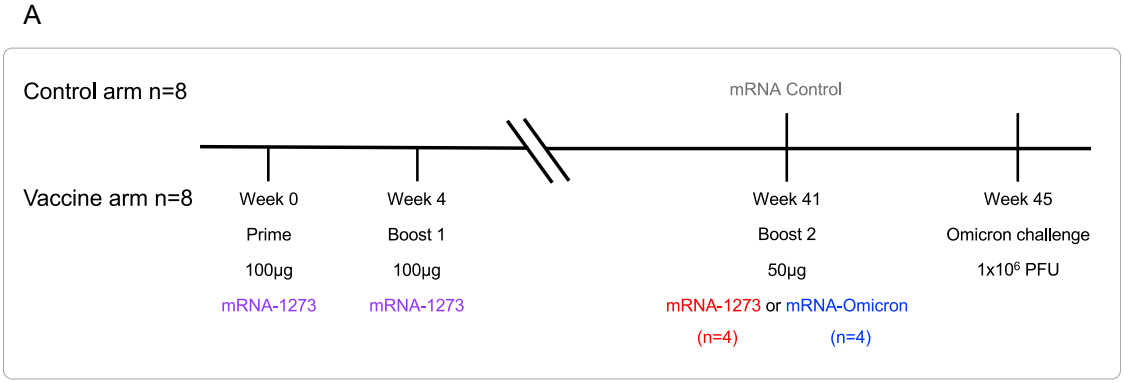

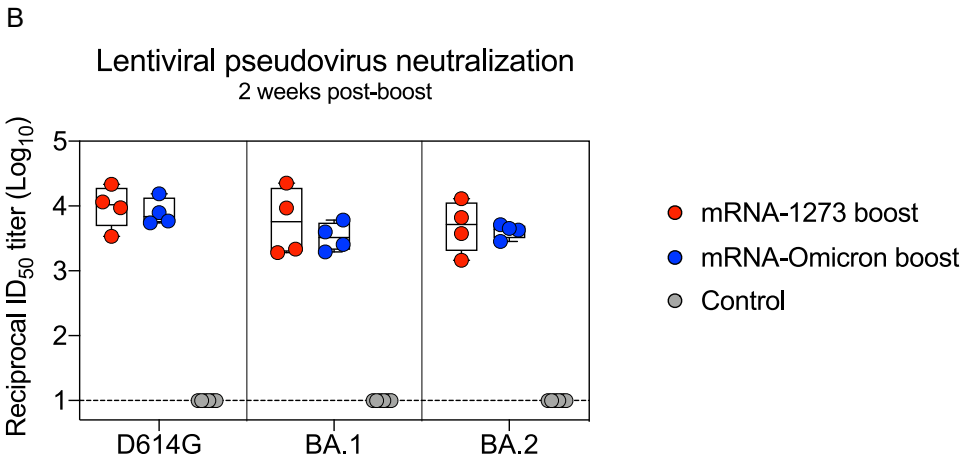

Figure S1. Experimental timeline and responses to Omicron sublineages after boost, related to Figure 1

(A) 8 NHP were vaccinated with 100 µg of mRNA-1273 at weeks 0 and 4. At week 41, NHP were split into 2 groups of 4 and boosted with 50 µg of mRNA-1273 or mRNA-Omicron. Both groups, and 8 unvaccinated NHP which were given 50 µg of mRNA control, were challenged with Omicron 1 month later.

(B) Sera were collected 2 weeks postboost to measure pseudoneutralizing responses to D614G and the BA.1 and BA.2 sublineages of Omicron. Circles indicate individual NHP. Boxes represent interquartile range with the median denoted by a horizontal line. Assay LOD indicated by dotted line. 4–6 NHP per group.

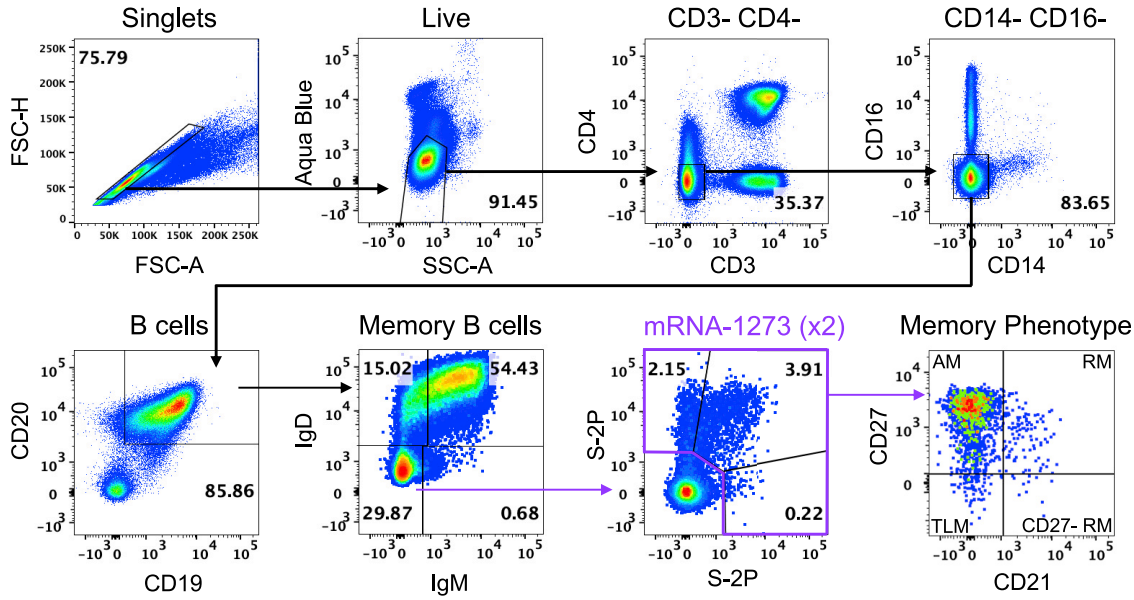

Figure S2. B cell-gating strategy, related to Figure 3

Representative flow cytometry plots showing gating strategy for B cells in Figures 3, 4, S3, and S5. Cells were gated as singlets and live cells on forward and side scatter and a live/dead aqua blue stain. CD3-, CD4-cells were then gated on absence of CD14 and CD16 expression and positive expression of CD20 and CD19. Memory B cells were selected based on lack of IgD or IgM. Finally, pairs of variant S-2P probes were used to determine binding specificity. Probe-binding cells were further characterized as having a phenotype consistent with CD27-negative resting memory (CD27-RM), tissue-like memory (TLM), activated memory (AM), or resting memory (RM) cells according to expression of CD27 and CD21.

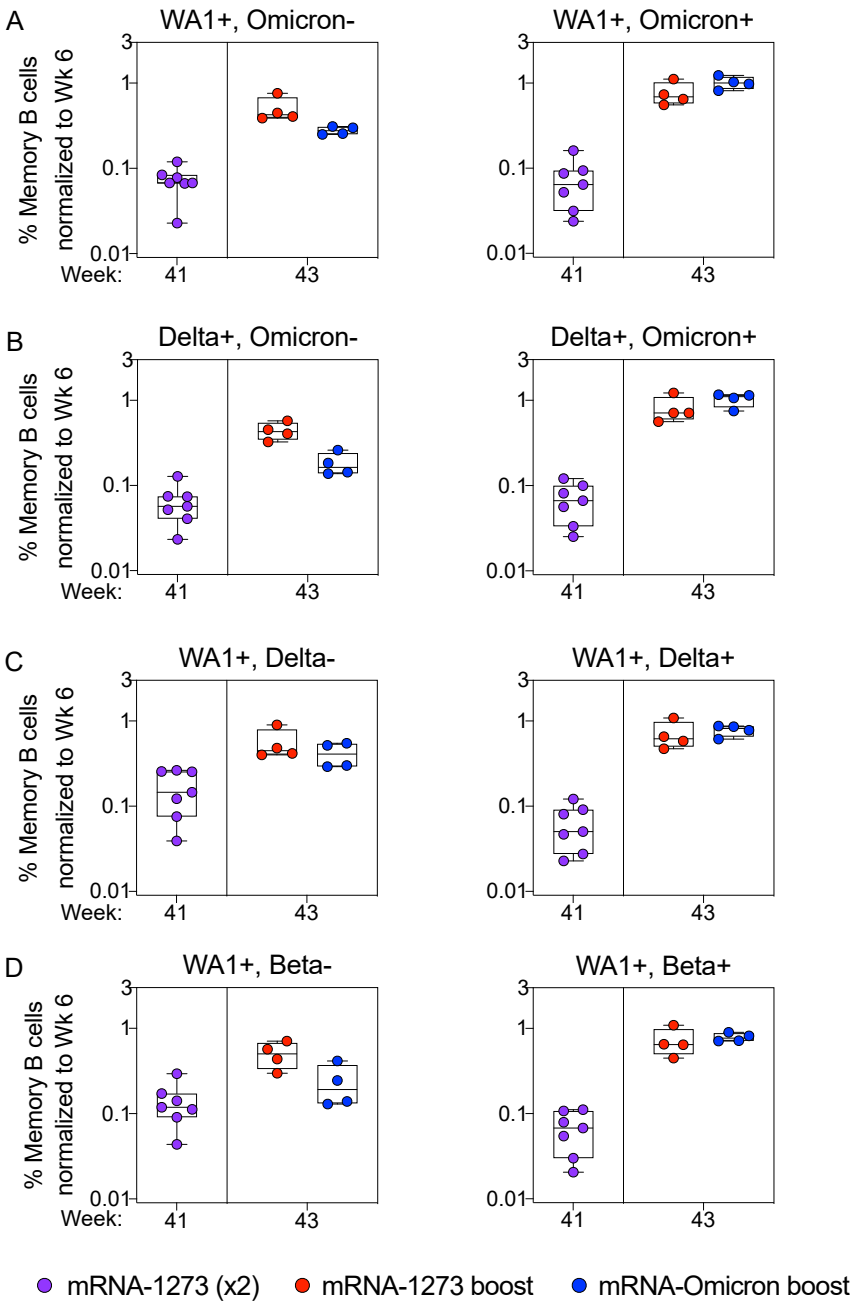

Figure S3. Expansion of memory B cells that recognize unique WA1 epitopes only occurs after homologous mRNA-1273 boosting, related to Figure 4

(A–D) Frequencies of memory B cells with indicated specificities as a percentage of total class-switched memory B cells (both S-2P-binding and non-S-2P-binding) were normalized to the corresponding frequencies from each individual NHP at week 6 post-immunization. Cross-reactivity shown for (A) WA1 and Omicron S-2P, (B) Delta and Omicron S-2P, (C) WA1 and Delta S-2P, and (D) WA1 and Beta S-2P. Specificities not shown if memory B cell populations were indistinguishable from background staining. Circles indicate individual NHP. Boxes represent interquartile range with the median denoted by a horizontal line. A frequency of 1 indicates parity. 4–7 NHP per group.

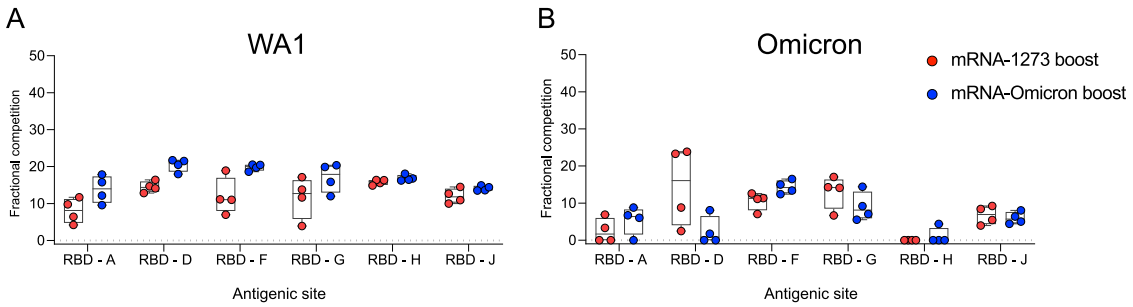

Site	A	D	F	G	H	J
mAb	B1-182	A19-46.1	A19-61.1	S309	A23-97.1	A23-80.1
				parent Ab of sotrovimab (Vir)		

Figure S4. Serum epitope reactivity following boost, related to Figure 4

(A and B) Relative serum reactivity was measured as fractional competition of total measured serum antibody S-2P binding competed by single monoclonal antibody (mAb) targeting epitopes on WA1 (A) or Omicron (B) S-2P at week 43 post-immunization. Antigenic sites are defined by mAbs B1-182 (RBD-A), A19-46.1 (RBD-D), A19-61.1 (RBD-F), S309 (RBD-G), A23-97.1 (RBD-H), and A23-80.1 (RBD-J). Circles indicate individual NHP. Boxes represent interquartile range with the median denoted by a horizontal line. Dotted lines are for visualization purposes and denote 0% competition. 4 NHP per boost group.

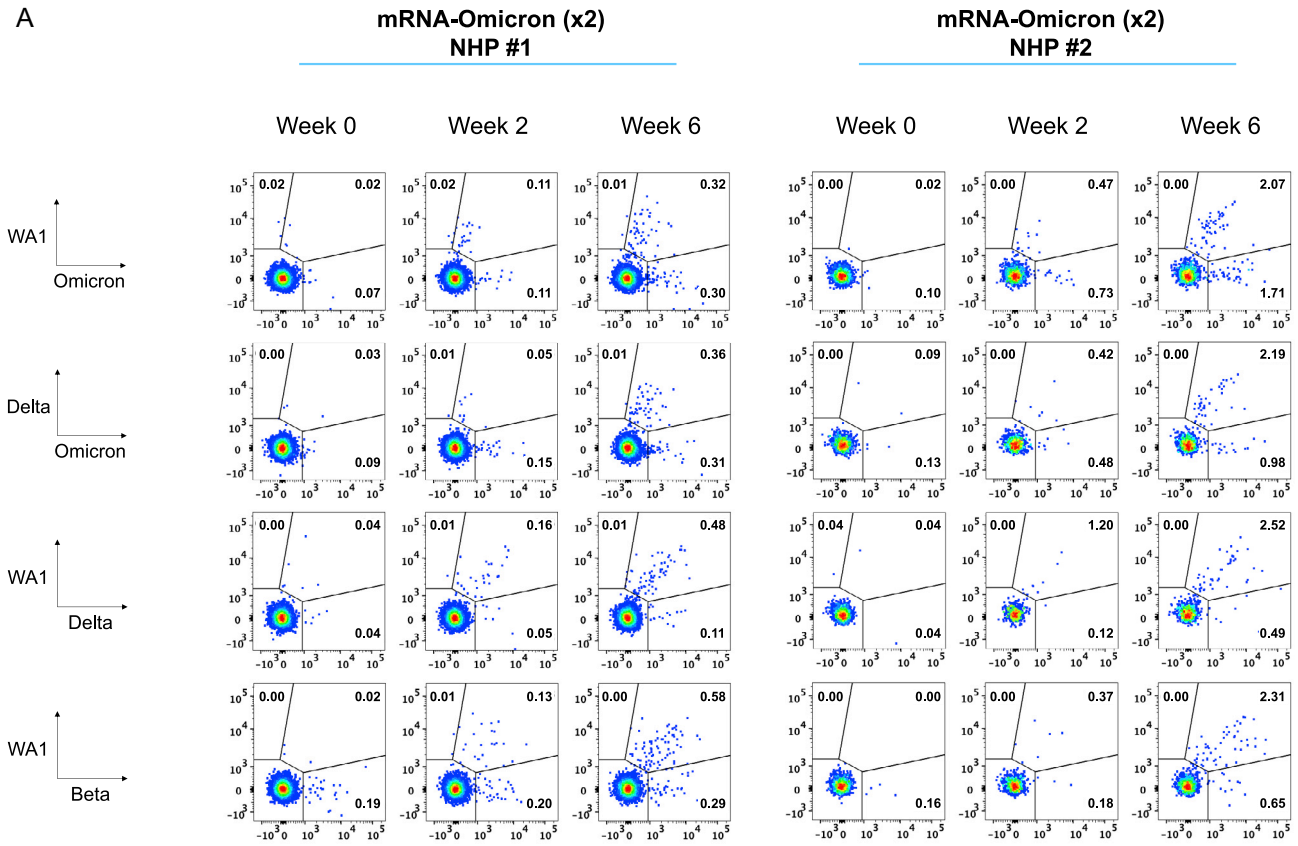

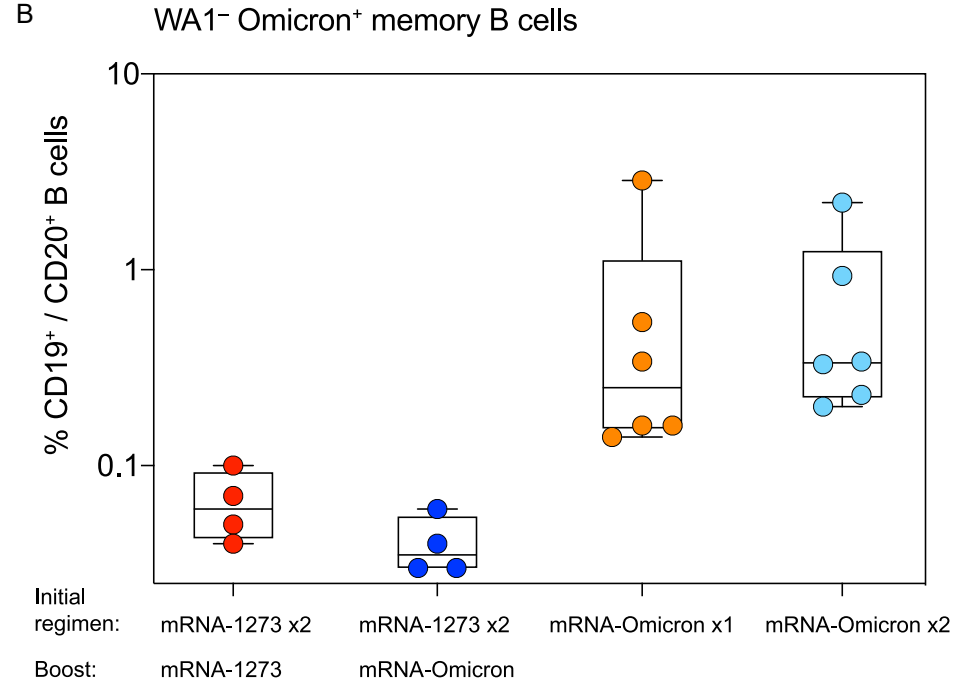

(legend on next page)

Figure S5. Memory B cell specificities following mRNA-Omicron immunization in naive primates, related to Figure 4

(A) Naive NHP were immunized with two doses of mRNA-Omicron (100 μg) at weeks 0 and 4. Representative flow cytometry plots for two different NHP showing single variant-specific (top left and bottom right quadrant) and dual-variant-specific (top right quadrant) memory B cells at weeks 0 (pre-vaccination) and 2 and 6 post-immunization. Event frequencies per gate are expressed as a percentage of all class-switched memory B cells. Cross-reactivity shown for WA1 and Omicron S-2P, Delta and Omicron S-2P, WA1 and Delta S-2P, and WA1 and Beta S-2P.

(B) Frequencies of memory B cells that bound Omicron S-2P but not WA1 S-2P as a percentage of total $CD19^+$, $CD20^+$ B cell population. Symbol colors are as follows: red (2 doses of 100 μg mRNA-1273 at weeks 0 and 4 and a 50 μg mRNA-1273 boost at week 41), blue (2 doses of 100 μg mRNA-1273 at weeks 0 and 4 and a 50 μg mRNA-Omicron boost at week 41), orange (1 dose of 100 μg mRNA-Omicron at week 0), and cyan (2 doses of 100 μg mRNA-Omicron at weeks 0 and 4). All analysis conducted 2 weeks after the final immunization for each cohort specified above. Circles indicate individual NHP. Boxes represent interquartile range with the median denoted by a horizontal line. 4–6 NHP per group.

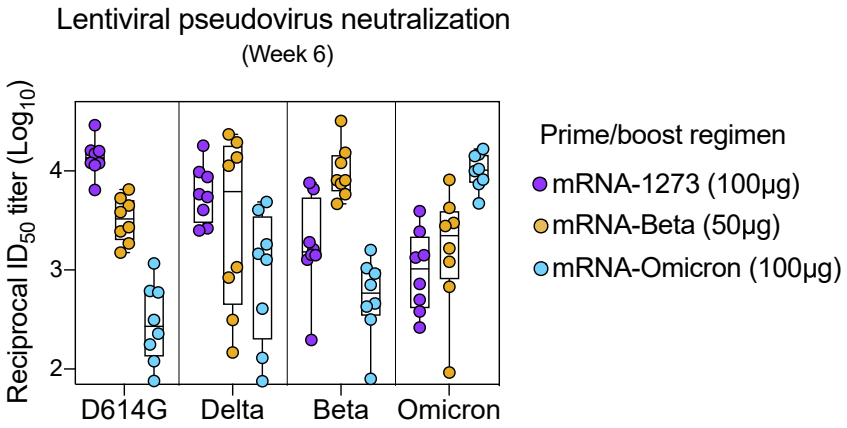

Figure S6. Primary responses to variant-matched vaccines, related to Figure 4

Naive NHP were immunized with two doses of mRNA-1273 (100 μg), mRNA-Beta (50 μg), or mRNA-Omicron (100 μg) at weeks 0 and 4. Sera were collected at week 6 to measure pseudoneutralizing responses to D614G, Delta, Beta, and Omicron. Circles indicate individual NHP. Boxes represent interquartile range with the median denoted by a horizontal line. Assay LOD (not shown) is 20. 8 NHP per cohort.

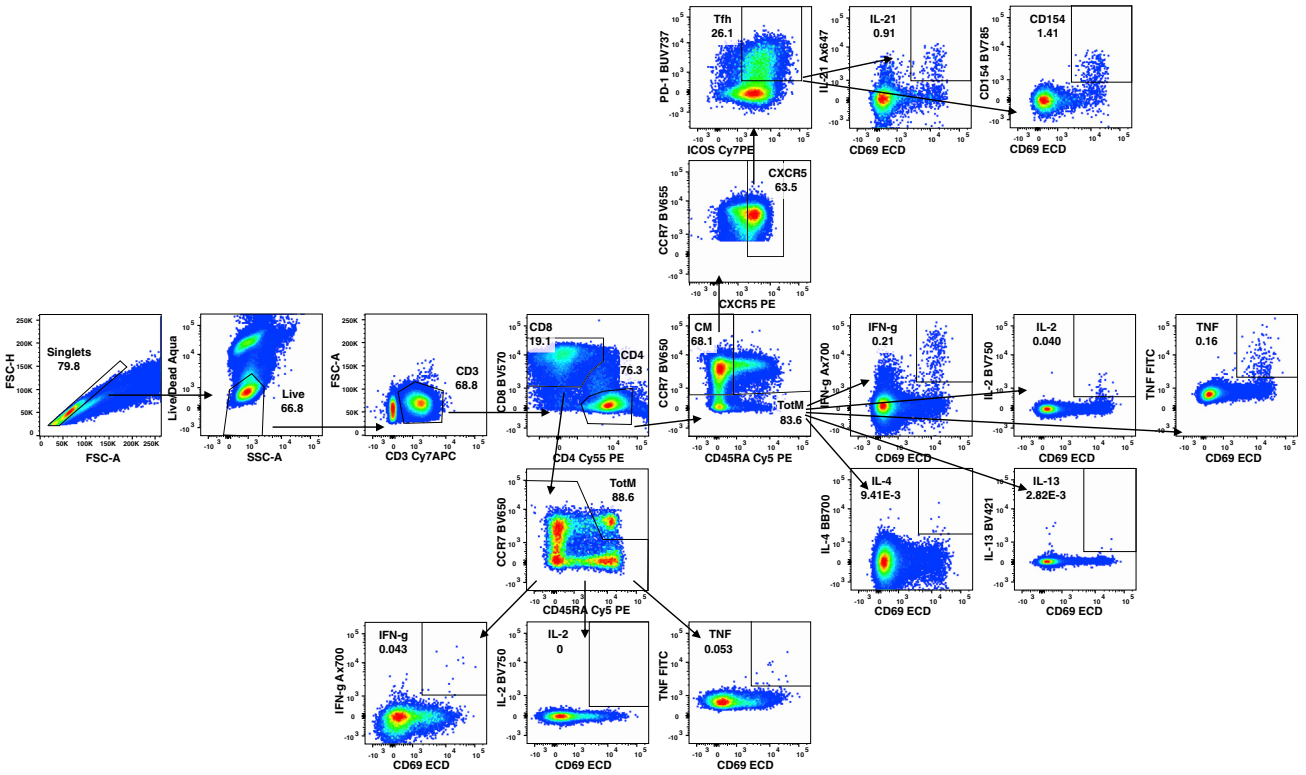

Figure S7. T cell-gating strategy, related to Figure 4

Representative flow cytometry plots showing gating strategy for T cells in Figures S8 and S9. Cells were gated as singlets and live cells on forward and side scatter and a live/dead aqua blue stain. CD3+ events were gated as CD4+ or CD8+ T cells. Total memory CD8+ T cells were selected based on expression of CCR7 and CD45RA. Finally, SARS-CoV-2 S-specific memory CD8+ T cells were gated according to co-expression of CD69 and IL-2, TNF or IFNγ. The CD4+ events were defined as naive, total memory, or central memory according to expression of CCR7 and CD45RA. CD4+ cells with a T_H1 phenotype were defined as memory cells that co-expressed CD69 and IL-2, TNF or IFNγ. CD4+ cells with a T_H2 phenotype were defined as memory cells that co-expressed CD69 and IL-4 or IL-13. T_{FH} cells were defined as central memory CD4+ T cells that expressed CXCR5, ICOS, and PD-1. T_{FH} cells were further characterized as IL-21+, CD69+ or CD40L+, CD69+.

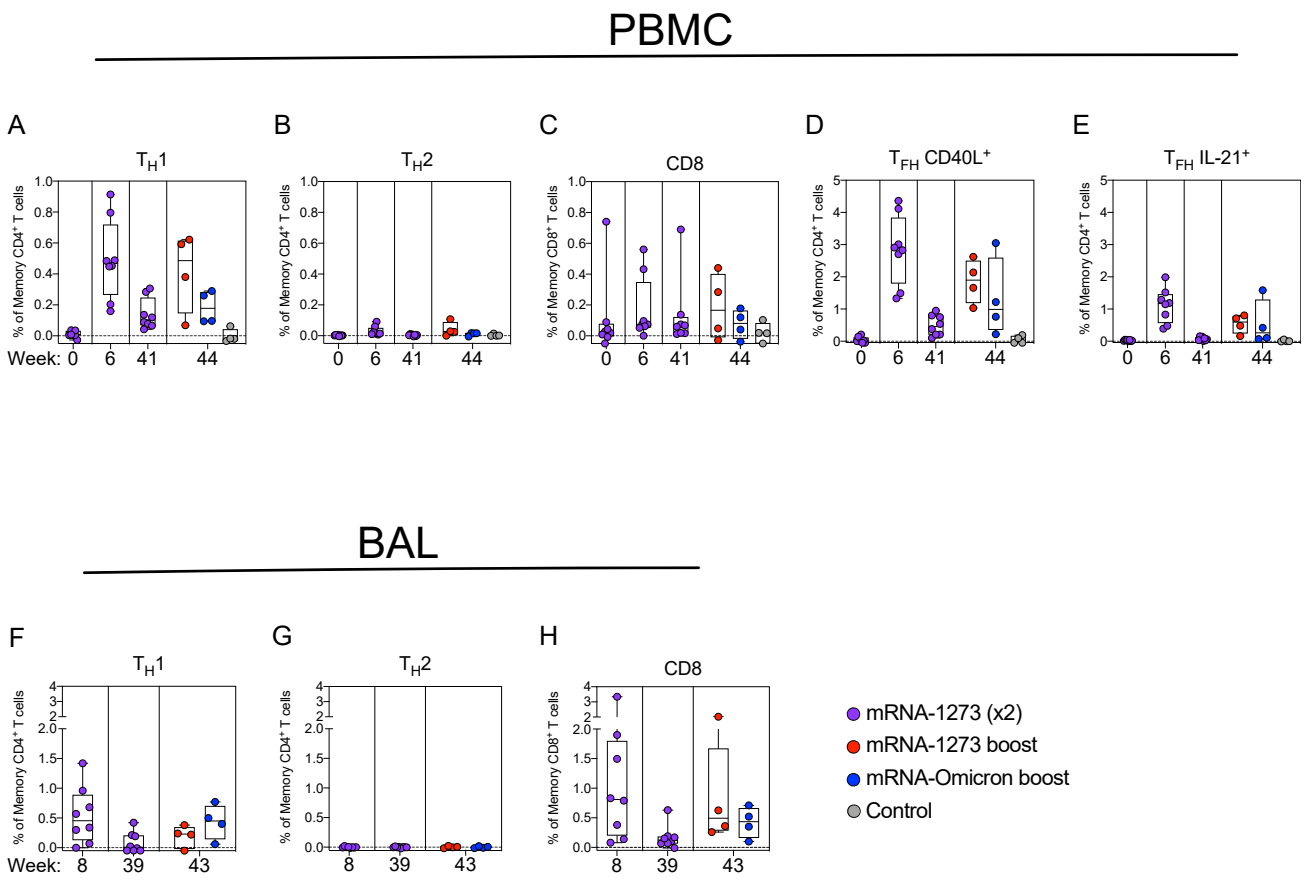

Figure S8. Both mRNA-1273 and mRNA-Omicron boost T cell responses to S peptides, related to Figure 4

(A–E) PBMC collected at weeks 0, 6, 41, and 44 post-immunization. Cells were stimulated with SARS-CoV-2 S1 and S2 peptide pools (WA1) and then measured by intracellular cytokine staining.

(A and B) Percentage of memory CD4+ T cells with (A) T_H1 markers (IL-2, TNF, or IFNγ) or (B) T_H2 markers (IL-4 or IL-13) following stimulation.

(C) Percentage of CD8+ T cells expressing IL-2, TNF, or IFNγ.

(D and E) Percentage of T_{FH} cells that express (D) CD40L or (E) IL-21.

(F–H) BAL fluid was collected at weeks 8, 39, and 43 post-immunization. Lymphocytes in the BAL were stimulated with S1 and S2 peptide pools (WA1) and responses measured by intracellular cytokine staining using T_H1 (F), T_H2 (G), and CD8 markers (H). Break in y axis indicates a change in scale without a break in the range depicted.

Circles in (A–H) indicate individual NHP. Boxes represent interquartile range with the median denoted by a horizontal line. Dotted lines set at 0%. Reported percentages may be negative due to background subtraction and may extend below the range of the y axis. 8 vaccinated NHP, split into 2 cohorts postboost. 4 control NHP shown for comparison.

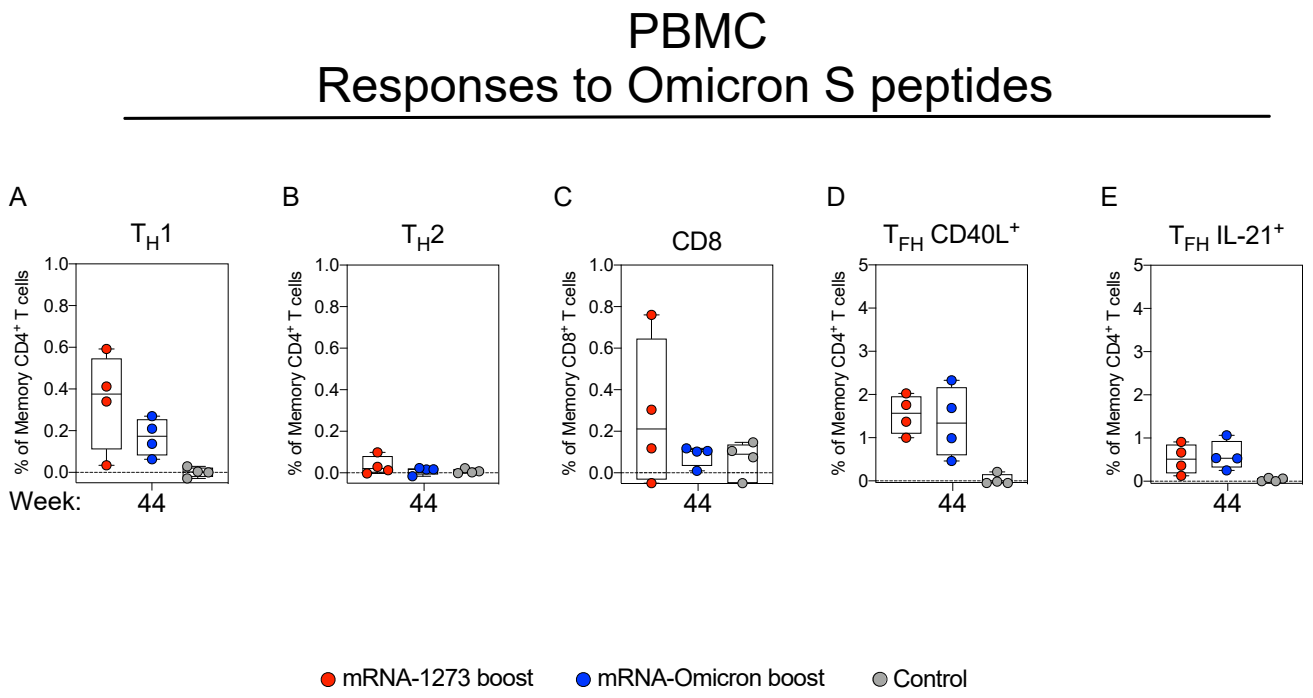

Figure S9. T cell responses to Omicron S peptides are conserved, related to Figure 4

(A–E) PBMC collected at week 44 post-immunization. Cells were stimulated with SARS-CoV-2 OS1 and OS2 peptide pools and then measured by intracellular cytokine staining.

(A and B) Percentage of memory CD4+ T cells with (A) T_H1 markers (IL-2, TNF, or IFNγ) or (B) T_H2 markers (IL-4 or IL-13) following stimulation.

(C) Percentage of CD8+ T cells expressing IL-2, TNF, or IFNγ.

(D and E) Percentage of T_{FH} cells that express (D) CD40L or (E) IL-21.

Circles in (A–E) indicate individual NHP. Boxes represent interquartile range with the median denoted by a horizontal line. Dotted lines set at 0%. Reported percentages may be negative due to background subtraction and may extend below the range of the y axis. 4 NHP per group.

A

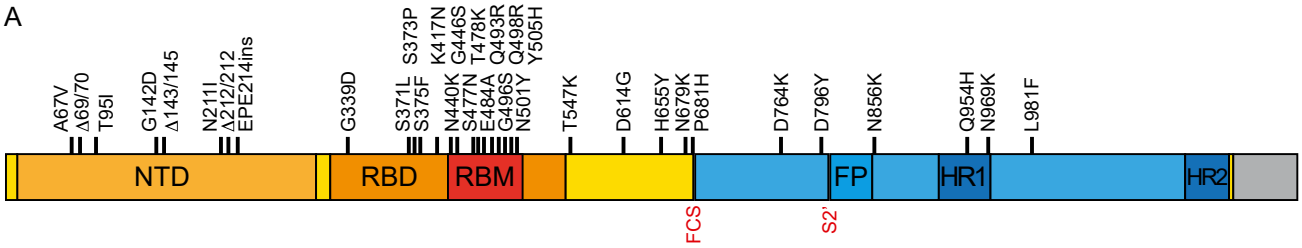

B

Gene	Amino acid change
ORF1ab	K856R
ORF1ab	S2083_L2084del insI
ORF1ab	A2710T
ORF1ab	T3255I
ORF1ab	P3395H
ORF1ab	L3674_G3676del
ORF1ab	I3758V
ORF1ab	P4715L
ORF1ab	I5967V
E	T9I
M	D3G
M	Q19E
M	A63T
N	P13L
N	E31_S33del
N	R203_G204del insKR

Figure S10. Omicron challenge stock sequence, related to Figure 5

(A and B) Omicron stock was sequenced and aligned with Wuhan-Hu-1.

(A) S gene only. Amino acid replacements listed above graphic. NTD, N-terminal domain; RBD, receptor binding domain; RBM, receptor binding motif; FP, fusion peptide; HR1, heptad repeat 1; HR2, heptad repeat 2; FCS, furin cleavage site; S2′, S2′ site.

(B) Whole genome.